MALARIA

The antimalarial MMV688533 provides potential for single-dose cures with a high barrier to *Plasmodium falciparum* parasite resistance

James M. Murithi[1†], Cécile Pascal[2†‡], Jade Bath[1], Xavier Boulenc[3‡], Nina F. Gnädig[1], Charisse Flerida A. Pasaje[4], Kelly Rubiano[1], Tomas Yeo[1], Sachel Mok[1], Sylvie Klieber[5], Paul Desert[3], María Belén Jiménez-Díaz[6], Jutta Marfurt[7], Mélanie Rouillier[8], Mohammed H. Cherkaoui-Rbati[8], Nathalie Gobeau[8], Sergio Wittlin[9,10], Anne-Catrin Uhlemann[11], Ric N. Price[7,12,13], Grennady Wirjanata[7], Rintis Noviyanti[14], Patrick Tumwebaze[15], Roland A. Cooper[16], Philip J. Rosenthal[17], Laura M. Sanz[18], Francisco Javier Gamo[18], Jayan Joseph[19], Shivendra Singh[19], Sridevi Bashyam[19], Jean Michel Augereau[2§], Elie Giraud[2‡], Tanguy Bozec[2‡], Thierry Vermat[2‡], Gilles Tuffal[5], Jean-Michel Guillon[2], Jérôme Menegotto[2‡], Laurent Sallé[5], Guillaume Louit[20], Marie-José Cabanis[5], Marie Françoise Nicolas[20], Michel Doubovetzky[2], Rita Merino[2‖], Nadir Bessila[2‡], Iñigo Angulo-Barturen[6], Delphine Baud[8], Lidiya Bebrevska[8], Fanny Escudié[8¶], Jacquin C. Niles[4], Benjamin Blasco[8#], Simon Campbell[8], Gilles Courtemanche[21], Laurent Fraisse[2¶], Alain Pellet[2‡], David A. Fidock[1,11]*, Didier Leroy[8]*

The emergence and spread of *Plasmodium falciparum* resistance to first-line antimalarials creates an imperative to identify and develop potent preclinical candidates with distinct modes of action. Here, we report the identification of MMV688533, an acylguanidine that was developed following a whole-cell screen with compounds known to hit high-value targets in human cells. MMV688533 displays fast parasite clearance in vitro and is not cross-resistant with known antimalarials. In a *P. falciparum* NSG mouse model, MMV688533 displays a long-lasting pharmacokinetic profile and excellent safety. Selection studies reveal a low propensity for resistance, with modest loss of potency mediated by point mutations in PfACG1 and PfEHD. These proteins are implicated in intracellular trafficking, lipid utilization, and endocytosis, suggesting interference with these pathways as a potential mode of action. This preclinical candidate may offer the potential for a single low-dose cure for malaria.

INTRODUCTION

Worldwide, malaria mortality and incidence were estimated to decrease by 60 and 37%, respectively, from 2000 to 2015. This positive trend came to an end in 2016, with cases and deaths plateauing, and 229 million cases and 409,000 deaths estimated in 2019 (*1*). *Plasmodium falciparum* parasite resistance to first-line artemisinin-based combination therapies continues to rise in Southeast Asia and now threatens Africa (*2*–*4*). Despite extensive global initiatives, malaria drug discovery and development efforts have encountered major obstacles to identifying chemical compounds with alternate modes of antiplasmodial action that do not readily succumb to parasite resistance (*5*).

To address these barriers, we applied an atypical drug discovery approach leveraging research and development programs on human diseases at Sanofi. Classical approaches rely on the identification of compounds that are both potent and specific against *Plasmodium* parasites, but our strategy first identified *Plasmodium*-active compounds from a library of chemical matter with known activity against human targets selected from discovery programs through to phase 3 clinical trials. Compounds active against *P. falciparum* asexual blood-stage parasites were then chemically optimized to increase antiplasmodial specificity and reduce host toxicity risks. Our approach led to the identification of several highly potent chemical series, including the acylguanidines that are exemplified by MMV688533. This molecule is shown herein to act via a previously undescribed mode of action that only allowed *P. falciparum* parasites to acquire low-grade resistance under drug pressure.

[1]Department of Microbiology and Immunology, Columbia University Irving Medical Center, New York, NY, USA. [2]Sanofi, Infectious Diseases Therapeutic Area, Marcy l'Etoile, France. [3]Sanofi Pasteur, Marcy L'Etoile, France. [4]Department of Biological Engineering, Massachusetts Institute of Technology, Cambridge, MA, USA. [5]Sanofi R&D, Translational Medicine & Early Development, Montpellier, France. [6]The Art of Discovery, Bizkaia, Basque Country, Spain. [7]Global and Tropical Health Division, Menzies School of Health Research and Charles Darwin University, Darwin, Australia. [8]Medicines for Malaria Venture, Geneva, Switzerland. [9]Department of Medical Parasitology and Infection Biology, Swiss Tropical and Public Health Institute, Basel, Switzerland. [10]Universität Basel, Basel, Switzerland. [11]Division of Infectious Diseases, Department of Medicine, Columbia University Irving Medical Center, New York, NY, USA. [12]Centre for Tropical Medicine and Global Health, Nuffield Department of Medicine, University of Oxford, Oxford, UK. [13]Mahidol-Oxford Tropical Medicine Research Unit, Faculty of Tropical Medicine, Mahidol University, Bangkok, Thailand. [14]Eijkman Institute for Molecular Biology, Jakarta, Indonesia. [15]Infectious Diseases Research Collaboration, Kampala, Uganda. [16]Department of Natural Sciences and Mathematics, Dominican University of California, San Rafael, CA, USA. [17]Department of Medicine, University of California, San Francisco, CA, USA. [18]Global Health Pharma Research Unit, GSK, Tres Cantos, Madrid, Spain. [19]Syngene International Ltd., Bangalore, India. [20]Sanofi, Vitry-sur-Seine, France. [21]Bioaster, Paris, France.
*Corresponding author. Email: df2260@cumc.columbia.edu (D.A.F.); leroyd@mmv.org (D.L.)
†These authors contributed equally to this work as co–first authors.
‡Present address: Evotec Infectious Diseases, Marcy L'Etoile, France.
§Present address: LCC-CNRS, 205 Route de Narbonne, 31400 Toulouse, France.
‖In memoriam.
¶Present address: Drugs for Neglected Diseases initiative, Geneva, Switzerland.
#Present address: Global Antibiotic Research and Development Partnership, Geneva, Switzerland.

RESULTS

Acylguanidines are potent antiplasmodial compounds with promising physicochemical properties

A bioinformatics-mediated analysis of Sanofi drug discovery programs led to the selection of 450 compounds active against one of 33 human targets for which putative orthologs were found in *P. falciparum*, *Trypanosoma brucei*, *Trypanosoma cruzi*, and/or *Leishmania donovani*. We also included 350 compounds active against any one of 28 Sanofi high-priority human targets. The screening of these 800 compounds against cultured *P. falciparum* asexual blood-stage parasites resulted in the identification of 120 compounds whose half-maximal growth inhibition concentration (IC_{50}) was ≤1 μM, corresponding to a 15% hit rate. As a comparison, classical random screening approaches have previously yielded 0.35 to 0.68% hit rates (*6*–*8*), highlighting a benefit of our drug discovery strategy. We then applied hit selection criteria including suitable physicochemical properties (www.mmv.org/research-development/information-scientists) and IC_{50} values <1 μM against a panel of drug-sensitive or -resistant *P. falciparum* strains and also screened an additional set of 800 analogs of preferred hits to expand the structure-activity relationships (SARs) (*9*). This work yielded six chemical scaffolds for medicinal chemistry optimization. Here, we describe the acylguanidine series, which includes the initial hit MMV668603 that was potent against *P. falciparum* NF54 asexual blood stages and had an IC_{50} of 1.7 nM. This hit originated from the dimerization of a compound chemically related to cariporide, an inhibitor of human Na^+/H^+ exchanger isoform 1 that has anticancer and cardioprotective properties (*10*, *11*). A hit to lead optimization program, including SAR studies, led to the intermediate compound MMV669851 and the eventual preclinical candidate MMV688533 (Fig. 1A). Compared with MMV668603, the candidate MMV688533 did not contain a diazo moiety, showed improved solubility (from <10 to >1000 μg/ml at pH 1) and intestinal permeability, and retained potent antiplasmodial activity (Fig. 1A and table S1, A and B).

MMV688533 displayed a fast asexual blood-stage parasite killing rate and high potency against *P. falciparum* and *P. vivax* strains in vitro and ex vivo

MMV688533 was highly potent against multiple *P. falciparum* strains, with IC_{50} values in the low nanomolar range and no evidence of reduced potency against parasite lines resistant to antimalarials currently in the clinic or in development (table S1C). These data suggest that MMV688533 might have a distinct mode of antiplasmodial action. MMV688533 also showed excellent ex vivo activity against asexual blood-stage parasites from fresh *P. falciparum* isolates from Ugandan patients (median IC_{50} = 1.3 nM, range = 0.02 to 6.3 nM, N = 143). In Papua Indonesia, where both *P. falciparum* and *P. vivax* are endemic, MMV688533 remained potent in ex vivo assays, with similar IC_{50} values against both parasite species (medians of 18.9 and 12.0 nM respectively; Table 1). MMV688533 was as potent as, if not more so than, either chloroquine or piperaquine against *P. falciparum* and *P. vivax* clinical field isolates (Table 1). This compound did not show potent activity against *P. falciparum* liver stages or male and female gametes (table S1D).

MMV688533 displayed a fast-killing profile in the parasite reduction ratio (PRR) assay (*12*), as demonstrated by a $\log_{10}$ PRR of nearly 5, corresponding to a decrease of parasitemia by nearly five orders of magnitude during a single 48-hour intraerythrocytic developmental cycle (Fig. 1B). Over 24 hours this profile is similar to dihydroartemisinin, the active metabolite of artemisinins that constitute the fastest-acting class of antimalarials available to date (*13*). This compound displayed very rapid parasite killing when tested over the range of 1× to 30× IC_{50} (Fig. 1C), as well as very low cytotoxicity (table S1E).

MMV688533 displayed fast and potent in vivo efficacy and favorable in vitro absorption, distribution, metabolism, and excretion and in vivo pharmacokinetic properties

MMV688533 was highly efficacious in the nonobese diabetic–severe combined immunodeficient NOD-scid interleukin-2Rγ^{null} (NSG) mouse model of *P. falciparum* asexual blood-stage infection (*14*), with a single oral dose of 5 mg/kg resulting in a rapid reduction in parasitemia to below the limit of detection within 48 hours, followed by recrudescence to 1% by day 18. By comparison, vehicle-treated mice attained a parasitemia of 8 to 10% by day 5 (Fig. 1D). These data predicted a 90% effective dose (ED_{90}) of 2 mg/kg, corresponding to the single dose required to reduce parasitemia by >90% by day 7 compared to vehicle-treated mice (Fig. 1, D and E, and table S1F). Four consecutive daily doses of 0.9 mg/kg produced >90% reduction in parasitemia by day 7. One dose of MMV688533 (at least 5 mg/kg) cleared parasites as rapidly as dihydroartemisinin (50 mg/kg; Fig. 1D). Pharmacokinetic-pharmacodynamic (PK/PD) modeling predicted an in vivo minimal parasiticidal concentration of 20.3 ng/ml (table S1G).

PK studies indicated a low plasma clearance (C_L) in mice, rats, and dogs (table S1H). When tested on purified cytochrome P450 enzymes, MMV688533 did not show high inhibitory potency (table S1I). MMV688533 also displayed a moderate to high volume of distribution (V_{ss}: 1.4 liters/kg in mice and 4.7 liters/kg in Beagle dogs) and a moderate to long half-life in all species (3.2 hours in mice and 50.7 hours in dogs) (table S1, J and N). The oral bioavailability of MMV688533 was >70% in rodent species (table S1J). Human C_L and V_{ss} parameters calculated from rat and dog allometry were predicted to be inferior to 5% of the hepatic blood flow using two methods (see Materials and Methods) and 540 liters for a 70-kg patient, respectively. The predicted half-life of MMV688533 in humans was greater than 100 hours (table S1P).

We then predicted an efficacious single dose in humans based on the following: (i) the minimal parasiticidal concentration derived from PK/PD modeling of the Pf NSG data (table S1, F and G); (ii) the K_{kill} derived from in vitro PRR studies (Fig. 1B); (iii) the PK in mouse, rat, and dog used in allometric scaling (table S1, J to P); and (iv) a biopharmaceutical model (GastroPlus). This latter model predicted that at least 50% of a 500-mg dose was absorbed when administered in fed conditions. A 100-mg dose was absorbed up to 70% in fasted conditions, while at this dose, the food effect was less than 30%. Using these parameters, a single oral administration of 30 mg of MMV688533 in humans would be predicted to maintain its concentration above the minimal parasiticidal concentration over a period of 96 hours, which covers two *P. falciparum* erythrocytic replication cycles, and to reduce parasitemia by at least 6 logs when a conservative in vitro log PRR value was capped at 3. Similarly, a dose of 24 mg is predicted to reduce parasitemia when the in vitro log PRR value of 5 was used. A single-dose treatment with 66 mg of MMV688533 is predicted to reduce parasitemia by 12 logs, suggesting very favorable characteristics for future clinical studies.

MMV688533 revealed a favorable tolerability profile

In silico toxicity predictions did not raise any safety alerts other than a moderate phototoxic risk (table S1Q), which proved minimal

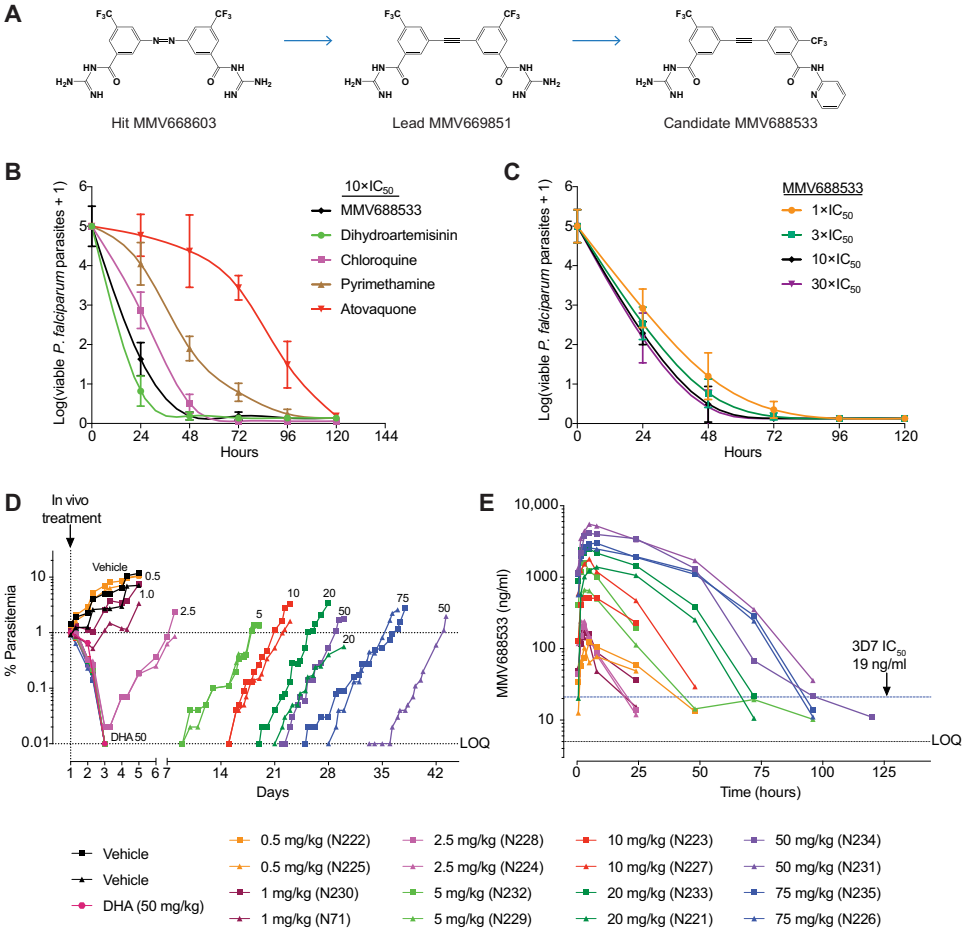

Fig. 1. The preclinical antimalarial candidate MMV688533 has a fast rate of antiplasmodial activity that offers potent single-dose activity against *P. falciparum* infection in a humanized mouse model. (**A**) Structural representation showing the optimization of the acylguanidine series from the initial hit MMV668603 and the lead MMV669851 to the candidate MMV688533. (**B**) Means ± SD values of viable *P. falciparum* parasites were determined daily for 5 days after in vitro incubation with MMV688533 at 10× the IC_{50}. Dihydroartemisinin, chloroquine, pyrimethamine, and atovaquone were included as reference antimalarial drugs. (**C**) Means ± SD values of *P. falciparum* viability determined daily for 5 days after MMV688533 treatment at doses corresponding to 1×, 3×, 10×, or 30× the IC_{50}. (**D**) Compound efficacy was assessed by measuring the initial clearance and time of recrudescence of *P. falciparum* in the peripheral blood of humanized mice that had been administered single doses of MMV688533 ranging from 0.5 to 75 mg/kg (two mice per dose). DHA (50 mg/kg) and vehicle were included as controls. (**E**) Concentration of MMV688533 in serial blood samples obtained after administering different doses to *P. falciparum*–infected humanized mice assayed in (D). LOQ, limit of quantification.

when tested in MMV688533-treated BALB/c 3T3 mouse fibroblasts exposed to ultraviolet light. Genotoxicity testing with MMV688533, including preliminary Ames and micronucleus assay, was negative. Profiled on a receptor/enzyme panel, MMV688533 displayed micromolar affinity for calcium and chloride channels as well as for benzodiazepine and dopamine receptors (table S1R). Considering its similarity with cariporide, cardiovascular parameters were assessed in detail. MMV688533 had a modest effect on the human Ether-à-go-go-Related Gene (hERG) channel with an IC_{50} of 30 and 4.6 μM when measured by automatic and manual patch clamp (table S1S), respectively. Inhibition studies with Nav1.5 and Cav1.1 ion channels yielded IC_{50} values of 14 and 2.1 μM, respectively (table S1S). When tested in the Purkinje fiber assay, MMV688533 induced mild effects that were not suggestive of a torsadogenic profile. However, because of the limited solubility of the compound in the conditions of this study, a full cardiosafety in vitro evaluation at higher concentrations was not possible. Therefore, in vivo studies were conducted to better assess potential cardiovascular safety risks. Continuous intravenous administration of MMV688533 (at 10, 20, and 30 mg/kg) to anesthetized guinea pigs did not affect blood pressure, heart rate, the electrocardiogram RR or QT intervals, or the QRS complex. In summary, in silico, in vitro, and in vivo safety studies with MMV688533 did not raise any measurable cardiotoxicity alerts.

Preliminary safety was assessed in rats and dogs via oral treatment and drug exposure measurements (toxicokinetics: table S1, T and U). In a non-Good Laboratory Practice (GLP) 2-week toxicity study in Sprague-Dawley rats, no clinically apparent changes were observed at 12.5, 25, and 50 mg/kg dose levels. In this study, 12.5 mg/kg per day exposure was considered the no-observed effect level (NOEL) due to an increase of liver biomarkers and microscopic changes (foamy macrophages and microscopic changes) at the two highest doses. In a non-GLP 2-week toxicity study in beagle dogs (0.5 and 1 mg/kg per day once daily and 2 mg/kg per day every other day), only minimal transient changes of no safety concern were detected. In conclusion, the no-observed-adverse-effect level (NOAEL) was declared at 1 mg/kg and the corresponding cumulated exposure over 14 days was 14-fold higher than that predicted for a 30-mg single dose in humans (table S1V). Such a predicted safety margin was judged promising enough to progress MMV688533 to more detailed regulatory preclinical studies before first-in-human clinical trials.

MMV688533 is maximally potent against *P. falciparum* rings and early trophozoite stages

To assess the timing of MMV688533 action, we used an in vitro asexual blood-stage susceptibility assay that measures compound activity against early and late rings, early and late trophozoites, and schizonts (*15*). The assay was validated by the stage-specific susceptibility profiles of dihydroartemisinin, chloroquine, and the PI4K inhibitor KAI407 (*16*), which showed the expected peak activities on early rings, rings and trophozoites, and schizonts, respectively (*15*). MMV688533 and dihydroartemisinin shared a similar activity profile,

Table 1. MMV688533 activity (in nanomolar) against *Plasmodium* parasite lines and field isolates. In vitro activity against *Plasmodium* culture-adapted lines or field isolates was calculated from dose-response curves and is shown as median or mean half-maximal growth inhibition (IC_{50}) in nanomolar concentrations. For the laboratory lines, numbers of independent repeats are shown in parentheses. 3D7 and FC27 are chloroquine sensitive, whereas Dd2 and K1 are chloroquine resistant. The potency of the other antimalarials was compared to MMV688533 using a Wilcoxon rank sum test.

	Laboratory lines	Laboratory lines	Laboratory lines	Laboratory lines	Clinical field isolates (Uganda)	Clinical field isolates (Papua, Indonesia)	Clinical field isolates (Papua, Indonesia)
	P. falciparum	*P. falciparum*	*P. falciparum*	*P. falciparum*	*P. falciparum*	*P. falciparum*	*P. vivax*
Antimalarial	3D7 (Median, *N*)	Dd2 (Median, *N*)	FC27 (Mean, *N*)	K1 (Mean, *N*)	Median (*N*; range)	Median (*N*; range)	Median (*N*; range)
MMV688533	1.9 (4)	3.0 (4)	9.7 (2)	19 (2)	1.3 (143; 0.02–6.3)	18.9 (15; 5.3–39.2)	12.0 (6; 5.4–19.9)
Chloroquine	11 (11)	347 (10)	10.9 (2)	100.3 (2)	17*** (143; 2.1–346)	64.8*** (15; 38.3–283)	36.4* (6; 11.6–114)
Piperaquine	4.4 (11)	7.9 (10)	25.8 (2)	111.2 (2)	5.1*** (140; 0.3–26)	60.8*** (15; 17.6–130)	46.6* (6; 15.0–135)
Mefloquine	4.8 (11)	6.6 (10)	37.2 (2)	8 (2)	8.3*** (120; 0.5–24)	10.0 (15; 4.9–41.9)	11.2 (6; 8.1–20.7)
DHA/artesunate†	1.9 (9)	1.7 (9)	0.6 (2)	1.1 (2)	1.5 (142; 0.1–9.0)	1.2*** (15; 0.4–4.3)	0.6* (6; 0.3–2.4)

*$P < 0.05$. ***$P < 0.001$. †DHA was tested on 3D7, Dd2, and Ugandan parasites, whereas artesunate was tested on FC27, K1 and Papua/Indonesian parasites.

with early rings to early trophozoites being the most susceptible, whereas schizonts were the least affected (Fig. 2A).

Ramping selections with *P. falciparum* asexual blood-stage parasites yield low-grade resistance to MMV688533

To identify possible resistance mechanisms to the acylguanidine MMV688533, we performed single-step in vitro resistance selections by exposing triplicate flasks of 2×10^9 wild-type Dd2-B2 parasites to 3× IC_{50} of MMV688533. These single-step selections did not yield resistant parasites after 60 days, suggesting a low propensity for resistance development for this compound. This was further confirmed in ramping selections, which entailed gradually increasing the drug pressure from 1 to 11× IC_{50} on triplicate flasks of 2×10^8 3D7-A10 parasites each over a 6-month period. This selection yielded only very low-grade resistance, with a two- to fivefold IC_{50} increase in each of the three drug-pressured lines (Fig. 2B and Table 2). Whole-genome sequencing (WGS) of four resistant clones obtained from across the three pressured lines identified single-nucleotide polymorphisms (SNPs) in five genes: a conserved *Plasmodium* protein of unknown function (PF3D7_0910300), an Eps15 homology domain (EHD)–containing protein (PF3D7_0304200), a conserved *Plasmodium* protein of unknown function (PF3D7_0510100), a putative RNA pseudouridylate synthase (PF3D7_0511500), and the putative adenosine 5′-triphosphate synthase (C/AC39) subunit (PF3D7_1464700) (Table 2 and table S2).

Of note, all four clones (sel. 533-CL1 to 533-CL4, named after the last three digits of the selecting compound MMV688533 followed by the clone name) carried G98V (clones sel. 533-CL1 and sel. 533-CL4), W286R (clone sel. 533-CL2), or T92* stop codon (clone sel. 533-CL3) mutations in PF3D7_0910300. These mutations were identified from three separately drug-pressured lines, suggesting a key role for this protein in conferring resistance to MMV688533. PF3D7_0910300, which we herein name *P. falciparum* acylguanidine 1 (PfACG1) in reference to the acylguanidine series, is a conserved *Plasmodium* protein of unknown function. Clone sel. 533-CL4, which also has a D218Y mutation in gene PF3D7_0304200 (PfEHD), displayed the highest level of resistance to MMV688533 (4.6-fold IC_{50} shift) (Fig. 2B and Table 2). This suggested an additional role for PfEHD in enhancing parasite resistance to the compound. On the basis of these observations, namely, the presence of PfACG1 mutations in all the selected clones and the apparent boost in resistance associated with an additional PfEHD D218Y mutation in sel. 533-CL4, we hypothesized that these two proteins, out of the five proteins identified using WGS, play a crucial role in mediating resistance to MMV688533. We chose to not assess the other three genes listed above as each harbored a mutation observed from only a single line, and unlike PF3D7_0304200, none of these three were associated with an increased degree of resistance (Table 2).

To test this hypothesis, we introduced the G98V and W286R mutations in PfACG1 and the D218Y mutation in PfEHD individually into wild-type 3D7-A10 parasites using a CRISPR-Cas9 gene-editing strategy. This yielded the edited lines ed. 3D7 $ACG1^{G98V}$, ed. 3D7 $ACG1^{W286R}$, and ed. 3D7 EHD^{D218Y}. The G98V mutation in the ed. 3D7 $ACG1^{G98V}$ line conferred comparable levels of resistance to the corresponding selected clone sel. 533-CL1, whereas the W286R mutation in the ed. 3D7 $ACG1^{W286R}$ line only contributed around half of the resistance observed in sel. 533-CL2 (Fig. 2B and Table 2). The D218Y mutation in PfEHD alone was insufficient to confer resistance. To test whether SNPs in PfACG1 are needed to obtain higher-grade resistance to MMV688533, we introduced the D218Y mutation into the background of the clone sel. 533-CL1, using a CRISPR-Cas9 strategy. This clone harbors the G98V mutation in PfACG1. The resulting sel. ed. 533-$CL1^{EHD\text{-}D218Y}$ line showed a 6.2-fold shift in IC_{50} compared to wild-type parasites, comparable to the 4.6-fold shift in clone sel. 533-CL4. These results provide evidence that the D218Y mutation in PfEHD enhances resistance to MMV688533 when the G98V mutation is already present in PfACG1.

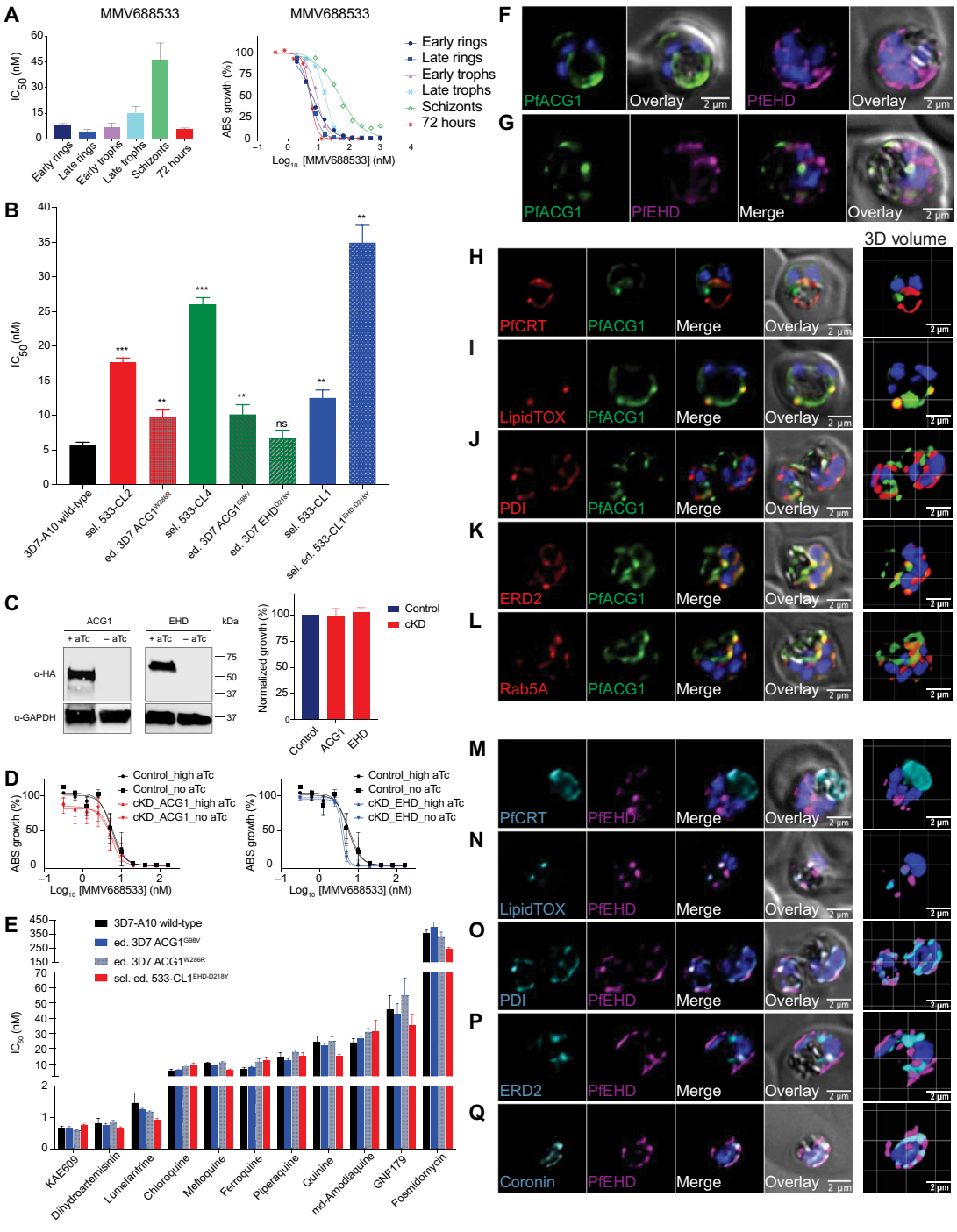

Fig. 2. MMV688533 antiplasmodial activity is unrelated to existing antimalarials and selects for low-grade resistance mediated in part by mutations in PfACG1 and PfEHD. (**A**) In vitro asexual blood-stage susceptibility assay showing MMV688533 activity in early and late rings, early and late trophozoites, and schizonts. IC_{50} values are shown as means ± SEM ($N > 3$, $n = 2$). (**B**) MMV688533 mean ± SEM IC_{50} values of selected (sel.) (533-CL1, 533-CL2, and 533-CL4), edited (ed.) ($PfACG1^{G98V}$, $PfACG1^{W286R}$, and $PfEHD^{D218Y}$) lines, and the sel. ed. line 533-$CL1^{EHD\text{-}D218Y}$ compared to the 3D7-A10 parental line. $N > 6$, $n = 2$; $^{**}P < 0.01$ and $^{***}P < 0.0005$; ns, not significant. (**C**) Western blot data showing effective reduction in PfACG1 and PfEHD protein levels upon removal of aTc, as detected using antibodies specific to the 2×HA tag added to the C terminus of each protein. Parasite survival was measured by quantifying expression of the integrated RLuc cassette (fig. S1), in the presence (50 nM) or absence of aTc. Data represent the mean of three biological replicates and are normalized to a fully inhibitory concentration of chloroquine (200 nM). (**D**) Dose-response curves for MMV688533 against PfACG1 and PfEHD ckD asexual blood-stage (ABS) parasites expressing wild-type or substantially reduced levels of each protein upon culturing with 500 nM aTc or no aTc, respectively. (**E**) G98V and W286R mutations in PfACG1 and a combination of both G98V in PfACG1 and D218Y in PfEHD in sel. ed. 533-$CL1^{EHD\text{-}D218Y}$ did not confer cross-resistance to a panel of known antimalarial drugs compared to the 3D7-A10 parent. Means ± SEM; $N > 3$, $n = 2$. (**F**) Fluorescence microscopy images of fixed $NF54^{3\times HA\text{-}EHD}$attB-ACG1-eGFP parasites stained with either anti-GFP (green) antibodies or anti-HA (magenta) antibodies. Nuclei were stained with DAPI (blue). Scale bars, 2 μm. (**G**) Fluorescence microscopy image of fixed and doubly stained $NF54^{3\times HA\text{-}EHD}$attB-ACG1-eGFP parasites using anti-GFP (green) and anti-HA (magenta) antibodies. Nuclei were stained with DAPI (blue). Scale bar, 2 μm. (**H** to **L**) Fluorescence microscopy images and 3D reconstructions of fixed $NF54^{3\times HA\text{-}EHD}$attB-ACG1-eGFP parasites costained with antibodies to anti-GFP (green) and (H) anti-PfCRT antibodies, (I) LipidTOX neutral lipid stain, (J) anti-PDI, (K) anti-ERD2, or (L) anti-Rab5A (red) antibodies. Nuclei were stained with DAPI (blue). Scale bars, 2 μm. (**M** to **Q**) Fluorescence microscopy images and 3D reconstructions of fixed $NF54^{3\times HA\text{-}EHD}$attB-ACG1-eGFP parasites costained with antibodies to anti-HA (magenta) and (M) anti-PfCRT antibodies, (N) LipidTOX neutral lipid stain, (O) anti-PDI, (P) anti-ERD2, or (Q) anti-coronin (cyan) antibodies. Nuclei were stained with DAPI (blue). Scale bars, 2 μm.

Table 2. Mutations identified in MMV688533-selected resistant *P. falciparum* clones and validated using CRISPR-Cas9 gene editing. Four parasite clones (sel. 533-CL1 from flask 1, sel. 533-CL2 and 533-CL3 from flask 2, and sel. 533-CL4 from flask 3) were generated from selections (sel.) and named after the last three digits of the selecting compound (MMV688533) followed by the clone number. These clones were then chosen for whole-genome sequencing. Fold IC_{50} increases compared to the parent 3D7-A10 are indicated below the clone names. *P. falciparum* ACG1^{W286R}, ACG1^{G98V}, and EHD^{D218Y} strains were gene-edited (ed.) using CRISPR-Cas9 to introduce the designated mutation into 3D7-A10 parasites. The sel. ed. 533-CL1$^{EHD\text{-}D218Y}$ clone was generated by CRISPR-Cas9 editing the EHD ^{D218Y} mutation into the selected 533-CL1 clone. wt, wild-type; ATP, adenosine 5′-triphosphate.

Gene product	Gene ID	Amino acid substitution							
		sel. 533-CL2	ed. 3D7 ACG1^{W286R}	sel. 533- CL3	sel. 533- CL4	ed. 3D7 ACG1^{G98V}	ed. 3D7 EHD^{D218Y}	sel. 533-CL1	sel. ed. 533-CL1$^{EHD\text{-}D218Y}$
		3.1 × IC_{50}	1.7 × IC_{50}	2.5 × IC_{50}	4.6 × IC_{50}	1.8 × IC_{50}	1.2 × IC_{50}	2.2 × IC_{50}	6.2 × IC_{50}
Conserved *Plasmodium* protein (PfACG1)	PF3D7_0910300	W286R	W286R	T92*	G98V	G98V	wt	G98V	G98V
EHD-containing protein (PfEHD)	PF3D7_0304200	wt	wt	wt	D218Y	wt	D218Y	wt	D218Y
Conserved *Plasmodium* protein	PF3D7_0510100	wt	wt	wt	wt	wt	wt	N1042H	N1042H
RNA pseudouridylate synthase, putative	PF3D7_0511500	wt	wt	K2762E	wt	wt	wt	wt	wt
ATP synthase (C/AC39) subunit, putative	PF3D7_1464700	L260I	wt	wt	wt	wt	wt	wt	wt

*Stop mutation resulting from a deletion-induced frameshift.

Conditional knockdown of the resistance determinants PfACG1 and PfEHD does not affect in vitro parasite growth

To further explore the role of PfACG1 and PfEHD, we engineered conditional knockdown (cKD) parasite lines in which we could regulate protein expression levels via the Tetracycline resistance Repressor - RNA helicase DOZI (development of zygote inhibited) (TetR-DOZI) System (*17*). Normal protein levels were maintained by culturing parasites in the presence of anhydrotetracycline (aTc) (fig. S1A). Western blot analysis of these lines, which harbored a C-terminal 2× hemagglutinin (HA) epitope tag fused to each gene product, confirmed the expression of PfACG1 and PfEHD in the presence of aTc (Fig. 2C and fig. S1B). aTc withdrawal resulted in the loss of protein expression, confirming efficient knockdown of the proteins. Despite the substantial knockdown observed from the Western blots, assessment of growth over two replicative cycles revealed that PfACG1 and PfEHD cKD parasites, maintained in the absence of aTc, were able to progress through the intraerythrocytic stage life cycle similar to controls. These results suggest that loss of function of either protein does not affect viability under normal culture conditions (Fig. 2C). To test for ex vivo compound-target interactions, we determined the IC_{50} of MMV688533 against wild-type versus knockdown conditions of PfACG1 and PfEHD. Knockdown of PfACG1 and PfEHD protein levels did not result in differential susceptibility to MMV688533 (Fig. 2D), providing evidence that these proteins are not directly targeted by MMV688533.

MMV688533-resistant parasites do not show cross-resistance to current antimalarials

To test whether resistance to MMV688533 might affect the efficacy of clinical antimalarials, we tested the 3D7 ACG1^{G98V} and 3D7 ACG1^{W286R} edited lines as well as the resistant clone sel. ed. 533-CL1$^{EHD\text{-}D218Y}$ for cross-resistance against a diverse panel of 11 known antimalarials. This study used 72-hour asexual blood-stage parasite susceptibility assays across a range of drug concentrations (Fig. 2E and table S3). Neither the individual G98V and W286R mutations in PfACG1 nor the multiple SNPs in sel. ed. 533-CL1$^{EHD\text{-}D218Y}$ conferred cross-resistance to these drugs, implying that MMV688533 has a different mode of action against *P. falciparum*.

PfACG1 and PfEHD localize primarily to distinct intracellular parasite vesicles

To interrogate the subcellular localization of PfACG1 and PfEHD, we performed immunofluorescence studies with a variety of cellular comarkers. We generated a doubly tagged recombinant NF54attB parasite line expressing a 3×HA tag at the C terminus of the PfEHD endogenous locus as well as a stably integrated transgenic copy of PfACG1 that was C-terminally tagged with enhanced green fluorescent protein (eGFP; NF54$^{3\times HA\text{-}EHD}$attB-ACG1-eGFP).

PfACG1-eGFP mainly localized to foci around the digestive vacuole (DV) of the parasite with residual labeling observed around the parasite nucleus (Fig. 2F and figs. S4 and S6). PfEHD likewise appeared in foci that localized mostly to the parasite periphery as well as close to the DV. Other foci were also other observed, although to a lesser extent, throughout the parasite cytoplasm (Fig. 2F and figs. S5 and S7). Colabeling using anti-HA and anti-GFP antibodies to assess colocalization of PfACG1 with PfEHD showed no overlap between the two fluorophores (Fig. 2G).

Most of the eGFP signal for the PfACG1-fusion protein was observed adjacent to the DV, so we performed costains using antibodies directed to *Plasmodium falciparum* chloroquine resistance transporter (PfCRT), *Plasmodium falciparum* multidrug resistance protein 1 (PfMDR1), or plasmepsin II, which are known to localize to this lysosome-like *Plasmodium* organelle (Fig. 2H and figs. S4, A and B, and S6, B and C). This confirmed some proximity to the DV, but imaging showed only infrequent and seemingly random overlap between PfACG1 and either of the DV transmembrane proteins PfCRT and PfMDR1. To investigate whether PfACG1 could overlap with neutral lipid bodies, which are often localized adjacent to the

parasite DV (*18*), we carried out costains using LipidTOX and Nile Red (Fig. 2I and fig. S4, C to F, and S6, D to G). Not all eGFP-positive foci exclusively overlapped with these lipid bodies, although we did observe frequent juxtaposition. These observations point to the possibility that PfACG1 partially associates with lipid storage bodies localized close to the DV.

Despite our detection of an eGFP signal close to the nucleus, no overlap was detected upon costaining for the parasite endoplasmic reticulum (ER) using antibodies specific for PDI (protein disulfide isomerase; Fig. 2J and fig. S6, H and I). Instead, the eGFP signal showed some overlap with antibodies to ERD2 and PMT (phosphoethanolamine *N*-methyltransferase), which represent markers for the cis- and trans-Golgi (*19*, *20*), respectively (Fig. 2K and figs. S4, G to J, and S6, J and K). To test whether PfACG1 localized to Rab-positive vesicles that are known mediators of vesicular traffic, we costained with Rab5A, Rab5B, and Rab7 antibodies. We observed infrequent overlap, similarly to costains performed with antibodies against K13, a marker for hemoglobin endocytosis (*21*, *22*) (Fig. 2L and figs. S4, K to N, and S6, L and O). Along these lines, no colocalization was observed for PfACG1 and coronin, a protein involved in F-actin organization that has recently been associated with in vitro resistance of early ring stages to artemisinins (*23*) (fig. S4O). Last, we assessed colocalization to the parasite mitochondrion using MitoTracker Deep Red, as well as to the apicoplast as visualized with anti–acyl carrier protein (ACP) antibodies. No overlap was observed between PfACG1-eGFP and those organelles (fig. S4, P and Q).

We detected PfEHD-positive foci that were close to the DV but did not colocalize with PfCRT, similar to our observations with PfACG1 (Fig. 2M and fig. S7, B and C). Costains using LipidTOX occasionally colocalized some of the HA-labeled PfEHD vesicles with neutral lipid bodies (Fig. 2N and figs. S5, A and B, and S7D). To test for possible PfEHD association with the parasite ER or the Golgi apparatus, we used antibodies directed to PDI, ERD2, or PMT. Frequent proximity and partial overlap were observed between PfEHD-positive foci and the ER-resident markers PDI and BIP, whereas the Golgi labeling (with ERD2 and PMT) revealed no obvious association between PfEHD and this organelle (Fig. 2, O and P, and figs. S5, C to F, and S7, E to H). In mammalian cells, EHD-containing proteins, serving as protein interaction platforms, are known to primarily function as key regulators in endocytosis (*24*). To explore whether PfEHD could play a similar role in protein and lipid trafficking processes in parasites, we performed immunofluorescence studies using antibodies to coronin and Rab proteins. We found that PfEHD vesicles that localized close to the parasite membrane frequently overlapped with coronin, hinting at a possible interaction between the two proteins (Fig. 2Q and figs. S5, G to J, and S7, I and J). Immunofluorescence assays carried out with the panel of Rab antibodies (anti-Rab5A, -Rab5B, -Rab5C, -Rab7, and -Rab11A) as well as antibodies to K13 revealed some juxtaposition of Rab-positive vesicles and K13-positive foci with PfEHD (figs. S5, L to P, and S7K). In contrast, when assessing potential PfEHD association with the apicoplast using anti-ACP antibodies, we did not observe overlap between the fluorophores (fig. S5Q).

DISCUSSION

Here, we report a potent antimalarial, MMV688533, developed after a whole-cell screen of Sanofi compounds active on defined human targets that were assayed for potency against *P. falciparum* asexual blood-stage parasites. Our screen of 800 compounds yielded a high hit rate, with 120 showing submicromolar antiplasmodial activity. Physicochemical analysis identified acylguanidines as the most promising series, with subsequent SAR-based lead optimization yielding MMV688533. PRR assays revealed rapid killing in vitro, with MMV688533 reducing the parasite load by >3 log within 24 hours after drug addition, similar to dihydroartemisinin and considerably faster than the comparator first-line drugs chloroquine and pyrimethamine. MMV688533 also displayed minimal toxicity against mammalian cells, slow clearance, and a long half-life, predicted at 100 hours in humans. Single-dose efficacy in the *P. falciparum*–infected NSG mouse model was excellent, with parasite clearance and delayed recrudescence observed at doses as low as 5 mg/kg. These data highlight the therapeutic potential of this class of antimalarials.

Whole-cell screens for antimalarials have yielded multiple potent antimalarials, which have encountered parasite resistance at frequencies and levels that pose a concern for their further development as curative drugs (*25*). For example, inhibitors of the drug targets PfATP4 or PfeEF2 can select for resistance from upwards of 10^7 parasites, with SNPs that can cause IC_{50} increases of a few up to several ten- or hundred–fold (*26*–*28*). In contrast, using these same selection procedures (*29*), MMV688533 yielded no resistance when used to pressure even large parasite inocula (6×10^9). Low-grade resistance could only be achieved by using a ramping method of gradually increasing drug concentrations over a 6-month period. Parasite clones from these selections showed two- to fivefold higher IC_{50} values against MMV688533. WGS identified two distinct point mutations or a stop codon in the PfACG1 gene in all clones assayed from three independent selections. Upon gene editing, both point mutations afforded only a twofold IC_{50} increase. One clone also harbored a point mutation in PfEHD, which, upon editing into a PfACG1 mutant line, resulted in a sixfold higher IC_{50} relative to the drug-sensitive 3D7 line. Other editing results showed that this PfEHD mutation on its own was insufficient to mediate parasite resistance. We note that three other genes were observed to each harbor a single nonsynonymous mutation. These mutations occurred separately in only one of the three flasks and may be attributable to stochastic events that arise naturally at low frequency during extended in vitro culture (*30*, *31*).

PfACG1 and PfEHD are both considered to be dispensable for *P. falciparum* asexual blood-stage growth in vitro (*32*), consistent with our cKD data in which no evident growth inhibition occurred despite virtually complete protein knockdown (Fig. 2C). PfACG1, previously annotated as a conserved protein of unknown function, is only conserved among Apicomplexan parasites of the genus *Plasmodium*, with minimal (~20%) amino acid identity to *Cryptosporidium andersoni* and *Cryptosporidium muris*. Protein sequence analysis shows a signal peptide at the N terminus and a single transmembrane domain at the C-terminal end. Little else is known about this protein. PfEHD contains a highly conserved EHD involved in protein-protein interactions and found in proteins that play a role in endocytosis (*24*). PfEHD has previously been linked to vesicular trafficking in *P. falciparum* parasites (*33*).

PfACG1 and PfEHD did not colocalize in our immunofluorescence assays. Nonetheless, PfACG1 colocalized with the neutral lipid markers LipidTOX and Nile Red, as well as the Golgi marker ERD2 that mediates protein retention in the ER and PMT that plays a critical role in phosphatidylcholine synthesis. These observations suggest that PfACG1 might play a role in vesicular trafficking or storage of lipids. In contrast, PfEHD showed some colocalization with the ER markers ERD2 and PDI as well as the actin-binding

protein coronin. PfEHD has previously been shown to be an interacting partner of AP-2μ, an adaptor protein that is essential for endocytosis and intracellular trafficking (*34*). Together, these data suggest that PfACG1 and PfEHD might be involved in related intracellular trafficking pathway(s) acted upon by MMV688533, which would be consistent with our observation that mutations in both proteins contributed to resistance to this compound. These results, along with lack of chemical-genetic interaction observed using the cKD lines (Fig. 2C), suggest that neither of these two proteins is the actual target and that they function instead as resistance mediators. These data suggest that MMV688533's mode of action involves inhibition of vesicular trafficking and/or lipid storage pathways. At present, this compound can be considered "targetless," a feature shared by multiple antimalarials in clinical use or advanced stages of development, including lumefantrine, quinine, artemisinin derivatives, OZ439, and KAF156 (*25*, *35*).

Further research is clearly required to define the mode of action of MMV688533. One limitation of our current study is that we did not define how PfACG1 and PfEHD mediate low-level resistance, nor did we establish the biological roles of these proteins during parasite intraerythrocytic development. Additional studies are also required to identify the cellular targets of MMV688533. Last, our dosing predictions for first-in-human study are based, in part, on allometric scaling of PK data from animal models and will benefit from further refinement after completion of phase 1 clinical trials.

In conclusion, we report that the acylguanidine MMV688533 has favorable fast-acting and long-lasting PK/PD properties. Drug selection studies showed that parasites could only acquire low-grade resistance with large inocula, and no cross-resistance was observed with established antimalarials or advanced preclinical candidates. These data suggest an alternate mode of action for MMV688533, which appears to involve lipid-associated intracellular trafficking of essential components. The promising preclinical therapeutic margin and low single doses predicted to be efficacious in humans should improve compliance and enable a low cost of goods.

MATERIALS AND METHODS

Study design

This study's objective was to harness the potential of compounds with known drug-like properties, which had earlier fueled discovery and development pipelines in several therapeutic areas, as a source of potential antimalarial candidates with previously undiscovered modes of actions. Screening against *P. falciparum* asexual blood-stage parasites led us to identify an acylguanidine chemical series with promising potency and physicochemical properties. Medicinal chemistry yielded analogs with improved parasite selectivity and PK properties. Prioritized compounds were assayed for in vivo efficacy in a humanized mouse model of *P. falciparum* infection. Preclinical toxicity studies with 4- or 14-day exposures were then performed in rats and dogs to predict a safety margin for clinical use. Cross-resistance and drug selection studies were used to test for resistance liabilities. cKD and gene-editing experiments, along with immunofluorescence imaging, were leveraged to conduct exploratory studies into compound mode of action. All assays were performed with multiple repeats with technical duplicates or triplicates, with positive and negative controls, as indicated in Materials and Methods and in figure legends.

MMV688533 synthesis

MMV688533 was synthesized as described in Supplementary Materials and Methods and illustrated in fig. S8.

Compound potency against *P. falciparum* and *P. vivax* parasites

Antimalarial activity against resistant culture-adapted strains of *P. falciparum* was measured with the modified [^{3}H]-hypoxanthine incorporation assay, as previously reported (*36*). Compounds, field locations, and sample collections are described in Supplementary Materials and Methods. Ex vivo potency assays against *P. falciparum* and *P. vivax* clinical isolates are described below.

In Papua Indonesia, drug susceptibility was measured in *P. vivax* and *P. falciparum* isolates using a protocol modified from the World Health Organization microtest (*37*–*39*). Briefly, 200 μl of a 2% hematocrit of blood media mixture, consisting of RPMI 1640 medium plus 10% AB$^+$ human serum for *P. falciparum* or McCoy's 5A medium plus 20% AB$^+$ human serum for *P. vivax*, was added to each well of predosed drug plates containing 11 serial concentrations (twofold dilutions) of the test antimalarials (maximum concentration shown in parentheses) chloroquine (2993 nM), piperaquine (1029 nM), mefloquine (338 nM), artesunate (49 nM), and MMV688533 (237 nM). A candle jar was used to mature the parasites at 37°C for 35 to 56 hours. Incubations were stopped when >40% of the ring-stage parasites had reached the mature schizont stage in the drug-free control wells, as determined by light microscopy. Parasite growth was quantified by nucleic acid staining, and parasitemias were measured using flow cytometry. Parasite growth was quantified for each drug concentration and normalized to the control well. The dose-response data were analyzed using nonlinear regression analysis, and the IC_{50} values were derived using an inhibitory sigmoid E_{max} model (In vitro Analysis and Reporting Tool; IVART7). Ex vivo IC_{50} data were only used from predicted curves where the E_{max} and E_0 were within 15% of 100 and 1, respectively. The drug plate quality was assured by running schizont maturation assays with the *P. falciparum* chloroquine-resistant strain K1 and the chloroquine-sensitive strain FC27. For data quality control, raw flow cytometry values were analyzed by two independent operators and compared. If the raw dose-response data derived by the two operators led to a marked shift in IC_{50} estimates for any of the drugs, they were reviewed and adjusted by a third operator. Ethical approval for this study was obtained from the Eijkman Institute Research Ethics Commission of the Eijkman Institute for Molecular Biology, Jakarta, Indonesia; the Human Research Ethics Committee of the Northern Territory Department of Health and Families; and the Menzies School of Health Research, Darwin, Australia.

In Africa, drug susceptibility was measured in *P. falciparum* isolates using a protocol summarized as follows: All MMV compounds were dissolved in dimethyl sulfoxide (DMSO) to a final concentration of 0.5 to 10 mM and stored at −20°C. On the day of assay, 2 μl of DMSO stock drug was diluted in 498 μl of complete RPMI media [RPMI 1640 medium supplemented with 25 mM Hepes, 0.2% $NaHCO_3$, 0.1 mM hypoxanthine, gentamicin (100 μg/ml), and 0.5% Albumax I (Invitrogen)]. Diluted drugs were not stored for longer than 24 hours. Drugs were serially diluted threefold in 96-well assay plates in complete media containing 0.4% DMSO, to a final volume of 50 μl, in columns 1 to 10. Column 11 contained drug-free controls, while column 12 contained uninfected red blood cell (RBC) controls. Parasitized whole-blood samples were washed three times with RPMI (without AlbuMAX) media at 37°C and then resuspended in

fresh RPMI media to a final hematocrit of 2%. One hundred fifty microliters of the parasite culture was added to each well into the assay plate for final parameters of 0.2% parasitemia and 2% hematocrit. Plates were incubated for 72 hours in a humidified modular incubator under a tri-gas mixture (5% O_2, 5% CO_2, and 90% N_2) at 37°C. Plates were then stained with SYBR Green I, and fluorescence was determined using a BMG Fluostar Optima plate reader at an excitation of 485 nm and an emission of 530 nm (*40*). Fluorescence data were curve-fitted to estimate IC_{50} values (GraphPad Prism 7). For each isolate, a Z′ factor was calculated from drug-free positive and negative controls (eight parasitized RBC wells and eight uninfected RBC wells, respectively).

P. falciparum culture-adapted lines

Asexual blood-stage parasites were cultured at 3% hematocrit in O^+ human erythrocytes in RPMI 1640 medium supplemented with 50 μM hypoxanthine, $NaHCO_3$ (2.25 g/liter), 2 mM L-glutamine, 25 mM Hepes, 0.5% (w/v) AlbuMAXII (Invitrogen), and gentamycin (10 μg/ml) at 37°C in flasks gassed with 5% O_2/5% CO_2/90% N_2. The *P. falciparum* 3D7-A10 and Dd2-B2 clones used for the selections and drug assays, as well as the NF54attB line used to express *pfacg1*-eGFP and *pfehd*-3×HA, have been previously reported (*15*, *41*, *42*).

Determination of the in vitro rate of killing (PRR)

As described in (*12*), the compound IC_{50} was determined via [^{3}H]-hypoxanthine incorporation. For PRR assays, 10^5 3D7A parasite cultures were exposed to MMV688533 at 10× IC_{50} for 120 hours. Drug treatment was renewed every 24 hours over the entire period. Parasite aliquots were taken from the treated cultures every 24 hours, with drug washout, throughout the 5-day treatment period. Freshly obtained human RBCs and new media were then added to the drug-free parasites, which were serially diluted in quadruplicate into 96-well plates. Growth in individual wells was detected after 3 and 4 weeks using [^{3}H]-hypoxanthine incorporation. The number of viable parasites was determined by the dilution down to which growth was observed. The rate of killing was represented by the log of viable parasites as a function of treatment duration. PRR was defined as the log-linear reduction of viable parasites over 48 hours.

Determination of efficacy and PK profiles in the Pf NSG mouse model

Assays used the *P. falciparum* Pf3D70087/N9 parasite line (*14*), which was propagated in 23- to 28-g female NOD-scid interleukin-2Rγ^{null} (NSG; Charles River, France) mice at The Art of Discovery (TAD).

For in vivo efficacy trials, immunodeficient female NSG mice were engrafted with a minimum of 40% human erythrocytes circulating in peripheral blood during the entire experiment. Each mouse was inoculated with a 50 to 75% hematocrit erythrocyte suspension (Basque Center of Transfusion and Human Tissues, Galdakao, Spain and Bank of Blood and Tissues, Barcelona, Spain) in RPMI1640 medium, 25% (v/v) decomplemented human serum, and 3.1 mM hypoxanthine. Intraperitoneal and/or intravenous (via tail lateral vein) injections were done once daily until the end of the drug administration period. Humanized NSG mice were infected with peripheral blood from CO_2-euthanized donor mice harboring 5 to 10% parasitemia. The humanized mice of the efficacy study were infected by inoculation of 0.3 ml of the infected-erythrocyte suspension by the lateral vein of the tail. For treatment, drug was administered at day 1 (~1% patent parasitemia) (P0) by oral gavage (volume 10 ml/kg of body weight). To measure the therapeutic response, 2 μl of peripheral tail blood from *P. falciparum*–infected mice was stained with antibodies to TER-119–phycoerythrin (a marker of murine erythrocytes; Miltenyi Biotec) and SYTO-16 (nucleic acid dye) and analyzed by flow cytometry (Attune NxT Acoustic Focusing Flow Cytometer, Invitrogen). Drug effect on circulating *P. falciparum* Pf3D70087/N9 parasites was assessed by microscopy (Giemsa-stained blood smears; 2 μl of blood samples was taken at 48 and 96 hours).

To assess the drug concentrations in mice, 25-μl samples of peripheral blood were taken at different times (usually 0.5, 1, 2, 4, 6, or 8 hours and 23 hours after the first dosing), mixed with 25 μl of MilliQ H_2O, and immediately frozen on a thermal block at −80°C. The treated mice that reached the limit of detection by standard flow cytometry (<0.01% from total circulating erythrocytes) were maintained until day 60 of the assay with a chimerism >50% of total circulating erythrocytes by regular injection of human erythrocytes every 3 or 4 days. During the follow-up period, 2-μl blood samples were taken every 2 or 3 days and analyzed by flow cytometry with a limit of quantification of 0.1%. The first day of parasitemia detection was recorded. The mice were deemed cured (free of detectable parasites) if no recrudescence was detected by day 60.

As biological controls, (i) parasite growth in untreated and/or vehicle-treated individuals was evaluated from days 1 to 5; (ii) the parasite burden was measured from days 1 to 5 of the assay in individuals treated with a fixed dose of a standard antimalarial; and (iii) the distribution of parasitemia at day 1 of the assay for all individual mice tested in the assay was compared to parasitemia distributions in previous experiments.

For data analysis, ED_{90} and area under the curve at the ED_{90} (AUC_{ED90}) were defined and calculated according to Angulo-Barturen *et al.* (*14*). ED_{90} is the effective dose in milligrams per kilogram that reduced parasitemia by 90% at day 5 compared to vehicle-treated mice. AUC_{ED90} is the average estimated daily exposure that reduced parasitemia from peripheral blood at day 5 of the assay by 90% compared to vehicle-treated mice. The ED_{90} was calculated by fitting the variable $Y = \log_{10}$ (parasitemia at day 5 of the assay) and the variable $X = \log_{10}$ (dose level in milligrams per kilogram) defined as an ordered pair for every individual of the study. The AUC_{ED90} was calculated by fitting the variable $Y = \log_{10}$ (parasitemia at day 5 of the assay) and the variable $X = \log_{10}$ (AUC of compound during the first 23 hours after the first drug administration, in ng·hour/ml] defined as an ordered pair for every individual of the study. The equation used to fit the data is Y = bottom + (top − bottom)/(1 + 10((logED_{50} − X) × Hill Slope)). The ED_{90} and AUC_{ED90} were calculated by interpolation of the X value that corresponded to antilog$_{10}$ [Y = "Top" − 1] in each respective best fitted curve (*14*).

The time of exposure in days (*te*) and the average concentration in blood (*C*; in nanograms per milliliter) for killing all *P. falciparum* parasites in mice were interpolated from a multivariate logistic regression. The fitted function links the dichotomic response variable termed the therapeutic response (*Tr*), which takes $Tr_i = 0$ if an individual shows recrudescence and $Tr_i = 1$ if no recrudescence was detected at day 60 of the assay, and the explanatory variables *te* and *C*. These parameters offered direct empirical estimates of the time of exposure and concentration in blood to kill a defined number of circulating parasites, which was typically 10^8 per mouse.

The regression formula is as follows: $P(Tr = 1|t_e, C) = \frac{1}{1 + e^{-(\alpha+\beta_1 t_e+\beta_2 C)}}$

Data were analyzed using GraphPad Prism 7.0 (GraphPad Software), Excel 2016 (Microsoft), and R free software (www.r-project.org). Phoenix WinNonlin v.7.0 (Certara) was used for PK noncompartmental analysis. Animal experiments performed at TAD were approved by the TAD Institutional Animal Care and Use Committee. The Committee is certified by the Biscay County Government (Bizkaiko Foru Aldundia, Basque Country, Spain) to evaluate animal research projects from Spanish institutions according to point 43.3 from Royal Decree 53/2013 (BOE-A-2013-1337). All experiments were carried out in accordance with European Directive 2010/63/EU. The results from the animal experiments are reported following Animal Research: Reporting of In Vivo Experiments (ARRIVE) guidelines (www.nc3rs.org.uk/arrive-guidelines), except for disclosure of business trade confidential information.

Prediction of the efficacious dose in humans based on Pf NSG mouse PK/PD

The prediction of the first efficacious dose in humans was based on the following: (i) minimum parasiticidal concentration (MPC) as evaluated from a population-based PK/PD modeling of experimental data from NSG mouse studies. One team at MMV used Monolix software, and another at Sanofi used a NonMem software to build a PK/PD model. Both teams reached a similar median estimate value of 20 ng/ml as the MPC; (ii) K_{kill} of the compound as deduced from in vitro logPRR (five in 48 hours). However, a conservative approach was recommended by MMV to use a capped value of 3 based on values observed for endoperoxides when tested in humans; (iii) predicted human PK parameters as determined by an allometric approach. For the allometric scaling of clearance from animal data, we used two methods: Mahmood rules and the Fixed exponent method. These led to the prediction of a low to a very low MMV688533 clearance in humans, 3.6 and 1.4 liters/hour, respectively, that corresponded to a total clearance of <5% of hepatic blood flow. This, in turn, corresponded to a predicted half-life of 103 and 277 hours, respectively, in humans. The volume of distribution (V_{dss}) relying on allometry method with an exponent of 1 was predicted to be as large as 540 liters for a 70-kg human; (iv) a biopharmaceutical model (GastroPlus) used to estimate Fa% versus dose in humans and verified on rat and dog PK data.

Evaluation of genotoxicity; PK studies in mice, rats, and dogs; safety pharmacology profiling; and patch clamp electrophysiological hERG assays

These are described in the Supplementary Materials.

P. falciparum stage-specificity assays

In vitro IC_{50} values were determined by incubating parasites for 72 hours across a range of 10 different concentrations of antimalarial compounds plus two no-compound controls. Stage specificity assays used a modified protocol with tightly synchronized parasites tested at different starting stages of the asexual blood-stage cycle (*15*).

P. falciparum resistance selections

Single-step selections for MMV688533 resistance used triplicate flasks of 2×10^9 Dd2-B2 parasites exposed to 5× to 14× the IC_{50} (25 to 80 nM) of MMV688533. Selections were terminated after 60 days because resistant parasites had not emerged. Ramping selections used triplicate flasks of 2×10^8 3D7-A10 parasites exposed to MMV688533 at concentrations that increased gradually from 1× to 10× the IC_{50} (5.5 to 60 nM) over a 6-month period. Resistant clones were obtained from bulk cultures of the ramping selections by limiting dilution, and four clones were selected for WGS. MMV688533 growth inhibition was determined by staining the parasites with SYBR Green and MitoTracker Deep Red (Life Technologies) followed by flow cytometry (Accuri C6, BD Biosciences) (*43*). IC_{50} values were derived from growth inhibition data using nonlinear regression (Prism 9.0, GraphPad). Unless stated otherwise, all drug assays were performed on at least four separate occasions (as biological repeats) with two technical replicates.

WGS analysis

The 3D7-A10 parent and MMV688533-resistant clones were subjected to WGS using an Illumina TruSeq DNA PCR (polymerase chain reaction)–Free library preparation protocol and a MiSeq sequencing platform, as previously described (*44*).

Genome editing

Mutations in PfACG1 and PfEHD that were identified from the in vitro selections were validated by engineering them into the parental 3D7-A10 line using an "all-in-one" pDC2-based CRISPR-Cas9 plasmid (*45*) (fig. S2A). The Cas9 in this plasmid is derived from *Streptococcus pyogenes*, has been codon-optimized for *P. falciparum*, and is under the expression of a calmodulin promoter. The plasmid also contains a human *dhfr* (h*dhfr*) selectable marker (that confers resistance to WR99210) under a *P. chabaudi dhfr-ts* (PcDT) promoter and the sequence encoding the guide RNA (gRNA) under a U6 promoter. gRNAs were selected using the online tool ChopChop based on their proximity to the mutation of interest, guanine-cytosine (GC) content, and the absence of poly adenine/thymine (A/T) tracts (http://chopchop.cbu.uib.no). The gRNA primers were annealed with Bbs I overhangs using PCR and cloned into a Bbs I–linearized pDC2 CRISPR-Cas9 vector. The donor templates, also supplied on the same plasmid, had >300 bp of homology flanking the mutation of interest. These fragments were first amplified by PCR and cloned into pGEM-T vectors to introduce shield mutations by site-directed mutagenesis. Shielded donor fragments were then amplified by PCR and cloned into the Eco RI/Aat II–linearized pDC2 CRISPR-Cas9 vector by In-Fusion cloning (Takara). Last, the plasmids were midiprepped for transfections.

Parasites were electroporated with purified circular plasmid DNA as previously described (*46*). Briefly, a 2.5-ml culture of 3D7-A10 or sel. 533-CL1 (≥5% rings) was washed and resuspended in 220 μl of 1× Cytomix. This mixture was then added to 50 μg of plasmid DNA and electroporated at a voltage of 0.31 kV and a capacitance of 950 μF inside 2-mm-gap cuvettes (Bio-Rad) using a Gene Pulser (Bio-Rad) (*47*). Starting 1 day after the transfections, the cultures were selected for 6 days with 2.5 nM WR99210 (*46*) and maintained thereafter in complete media until recrudescence. Gene editing was assessed via Sanger sequencing of blood PCR (Bioline) from bulk cultures. Edited parasite clones were obtained by limiting dilution. The parasites were then assayed for resistance to MMV688533 using flow cytometry.

Both the mycobacteriophage Bxb1 serine integrase system (*47*) and CRISPR-Cas9 gene-editing tools were used to generate the doubly tagged parasite line expressing PfACG1-eGFP and PfEHD-3×HA fusion proteins. Briefly, NF54attB parasites (*41*) were first cotransfected with an integrase-expressing plasmid pINT and a donor attP-containing plasmid pDC2-*pfacg1*-eGFP. This donor plasmid also contained a blasticidin-*S* deaminase (BSD) selectable marker that

confers resistance to blasticidin hydrochloride (*48*). The integrase plasmid pINT contained a Neomycin selectable marker that confers resistance to geneticin [G418 (*49*); fig. S2B]. Transfections were done as described above, and the cultures were maintained in G418 (250 μg/ml) + BSD media (2 μg/ml) for 6 days after transfection, followed by BSD media (2 μg/ml) until recrudescence. Sorbitol-synchronized eGFP-tagged ring-stage clonal parasites obtained by limiting dilution were then transfected with the codon-optimized all-in-one plasmid containing a 1.1-kb *pfehd* donor fragment consisting of two 3′ homology sequences flanking the 3×HA tag (fig. S2C). These transfections were selected with 2.5 nM WR99210 (*50*) until recrudescence. Successful gene tagging was confirmed via PCR, Sanger sequencing, and immunofluorescence assays.

cKD parasite studies

Generation of cKD parasite lines

To investigate the interaction between MMV688533, PfACG1, and PfEHD, we used CRISPR-Cas9 to generate parasite cell lines stably expressing the TetR-DOZI-RNA aptamer module for conditional regulation of target gene expression. These transgenic lines also contained the reporter construct *Renilla* luciferase (RLuc), the selection marker BSD, and a C-terminal 2×HA epitope tag (*17*). To construct the donor plasmids, PCR-amplified right homology regions and BioXP3200 System–synthesized DNA fragments corresponding to the left homology regions fused to the recodonized 3′-end of each target gene, as well as the target-specifying gRNA sequences, were cloned via Gibson assembly into the pSN054 linear vector (*51*). The final constructs were confirmed by restriction digests and Sanger sequencing. Transfections into Cas9- and T7 RNA polymerase–expressing NF54 parasites were carried out by preloading erythrocytes with the donor plasmids as described previously (*52*). Cultures were maintained in 500 nM aTc (Sigma-Aldrich, 37919) and blasticidin-*S* (2.5 μg/ml; RPI Corp B12150-0.1). Parasite cell lines stably integrating the donor plasmids were monitored via Giemsa smears and RLuc measurements.

Western blotting of cKD parasite lines

PfACG1 and PfEHD cKD parasites were cultured with 50 nM aTc or without aTc to maintain and down-regulate protein expression, respectively. Proteins were then extracted after 72 hours via saponin lysis and resuspended in lysis buffer that consists of 4% SDS and 0.5% Triton X-114 in 1× PBS. Proteins were separated on Mini-PROTEAN TGX precast gels (4 to 15% gradient) in tris-glycine buffer, transferred to a polyvinylidene fluoride membrane using the Mini Trans-Blot Electrophoretic Transfer Cell System, and blocked with skim milk (100 mg/ml) in TBS/Tween. Membrane-bound proteins were probed with mouse anti-HA (1:3000; Sigma-Aldrich H3663) and rabbit anti–glyceraldehyde-3-phosphate dehydrogenase (1:5000; Abcam AB9485) primary antibodies and anti-mouse (1:5000; Thermo Fisher Scientific 62-6520) and anti-rabbit (1:5000; Cell Signaling Technology 7074S) horseradish peroxidase–conjugated secondary antibodies. After incubation in SuperSignal West Pico Chemiluminescent substrate (Thermo Fisher Scientific PI34080), protein blots were imaged and analyzed using the ChemiDoc MP System and Image Lab 5.2.0 (Bio-Rad).

cKD proliferation assays

To assess the effect of conditionally perturbing PfACG1 and PfEHD expression on parasite growth, synchronous ring-stage parasites cultured in the presence (50 and 3 nM) or absence of aTc were cultured in triplicate in a 96-well U-bottom plate (Corning, 62406-121). Luminescence signals were taken at 0, 72, and 120 hours after invasion using the Renilla-Glo(R) Luciferase Assay System (Promega E2750) and the GloMax Discover Multimode Microplate Reader (Promega). The luminescence values in the knockdown conditions were normalized to aTc-treated (100% growth) and chloroquine-treated (200 nM) samples (no growth) as controls and results were analyzed using GraphPad Prism (version 8; GraphPad Software).

Compound susceptibility assays with cKD parasite lines

A stock solution of MMV688533 was dispensed into 96-well U-bottom plates and serially diluted in complete medium to yield final concentrations ranging from 0.3 to 160 nM. Synchronous ring-stage PfACG1 and PfEHD cKD parasite lines, as well as a control cell line expressing an aptamer-regulatable fluorescent protein, were maintained in the presence (500 nM) or absence of aTc and were distributed into the drug plates. DMSO- and chloroquine-treated samples (200 nM) served as reference controls. Luminescence was measured after 72 hours as described above, and median effective concentration (EC_{50}) values were obtained from corrected dose-response curves using GraphPad Prism.

Immunofluorescence assays

Indirect immunofluorescence studies were performed in suspension. Cells were fixed in 4% (v/v) formaldehyde (Thermo Fisher Scientific) for 1 hour at room temperature, followed by a second fixation step supplementing the 4% formaldehyde solution with 1 mM cysteine and $CaCl_2$ and subsequent incubation overnight at 4°C. Cells were then permeabilized on ice using 0.05% Triton X-100 in 1× PBS for 5 min. Autofluorescence was quenched using a 50 mM glycine treatment for 10 min. After two washes in 1× PBS, the cells were resuspended in 1% (w/v) bovine serum albumin (BSA) in 1× PBS blocking buffer and were then incubated with the appropriate dilution for each primary antibody used: 1:200 for rabbit anti-ERD2 (BEI Recourses), anti-PMT (provided by C. B. Mamoun), anti-PDI [mouse anti-PDI (1D3), Enzo Life Sciences], rabbit or mouse anti-GFP [Takara (Clontech), Roche], and rabbit anti-HA antibodies (Sigma-Aldrich); 1:50 for rabbit anti-Rab5A, -Rab5C, or -Rab11A and rat anti-Rab5B or Rab7 (provided by G. Langsley); 1:200 for anti-coronin (provided by J. Baum); 1:200 for anti-ACP (provided by G. McFadden); 1:200 for anti-K13 (*22*); and 1:200 for anti-PfCRT antibodies (*53*), followed by incubation with corresponding species-specific secondary antibodies (Alexa Fluor 488–, 594–, or 647–conjugated goat anti-mouse or -rabbit antibodies; Thermo Fisher Scientific) diluted 1:2000 in 1% BSA in 1× PBS. MitoTracker Red CMXRos (Thermo Fisher Scientific) was used to stain mitochondria. HCS LipidTOX Deep Red Neutral Lipid Stain and Nile Red (Invitrogen) were used to stain neutral lipid bodies according to the protocol provided by the manufacturer. Thin blood smears of stained RBCs were prepared on microscope slides and mounted with coverslips using Prolong Diamond Antifade Mountant with 4′,6-diamidino-2-phenylindole (DAPI; Thermo Fisher Scientific). Parasites were imaged using a Nikon Eclipse Ti-E wide-field microscope equipped with an sCMOS camera (Andor) and a Plan-apochromate oil immersion objective with 100× magnification (1.4 numerical aperture). A minimum of 27 Z-stacks (0.2-μm step size) were photographed for each parasitized RBC. NIS-Elements imaging software (Version 5.02, Nikon) was used to control the microscope and camera, deconvolve the images (using 25 iterations of the Richardson-Lucy algorithm for each image), and perform 3D reconstructions (*22*). ImageJ (Fiji) (version 2.0.0-rc-68/1.52h) was used to crop the images, adjust brightness and intensity, overlay channels, and prepare montages.

Statistical analysis

Mann-Whitney *U* tests were performed (using Prism 9.0; GraphPad) to test for statistical significance between isogenic parasite lines in their drug IC_{50} values (Fig. 2B and table S3). Wilcoxon rank sum tests were used to identify significant differences in drug susceptibility between *P. falciparum* field isolates (Table 1).

SUPPLEMENTARY MATERIALS

stm.sciencemag.org/cgi/content/full/13/603/eabg6013/DC1
Materials and Methods
Figs. S1 to S8
Tables S1 to S3
Raw Data Spreadsheet
References (*54*–*67*)

View/request a protocol for this paper from *Bio-protocol*.

REFERENCES AND NOTES

1. WHO, World Health Organization. World malaria report 2020; www.who.int/teams/global-malaria-programme/reports/world-malaria-report-2020.
2. M. D. Conrad, P. J. Rosenthal, Antimalarial drug resistance in Africa: The calm before the storm? *Lancet Infect. Dis.* **19**, e338–e351 (2019).
3. M. Imwong, M. Dhorda, K. Myo Tun, A. M. Thu, A. P. Phyo, S. Proux, K. Suwannasin, C. Kunasol, S. Srisutham, J. Duanguppama, R. Vongpromek, C. Promnarate, A. Saejeng, N. Khantikul, R. Sugaram, S. Thanapongpichat, N. Sawangjaroen, K. Sutawong, K. T. Han, Y. Htut, K. Linn, A. A. Win, T. M. Hlaing, R. W. van der Pluijm, M. Mayxay, T. Pongvongsa, K. Phommasone, R. Tripura, T. J. Peto, L. von Seidlein, C. Nguon, D. Lek, X. H. S. Chan, H. Rekol, R. Leang, C. Huch, D. P. Kwiatkowski, O. Miotto, E. A. Ashley, M. P. Kyaw, S. Pukrittayakamee, N. P. J. Day, A. M. Dondorp, F. M. Smithuis, F. H. Nosten, N. J. White, Molecular epidemiology of resistance to antimalarial drugs in the Greater Mekong subregion: An observational study. *Lancet Infect. Dis.* **20**, 1470–1480 (2020).
4. A. Uwimana, E. Legrand, B. H. Stokes, J.-L. M. Ndikumana, M. Warsame, N. Umulisa, D. Ngamije, T. Munyaneza, J.-B. Mazarati, K. Munguti, P. Campagne, A. Criscuolo, F. Ariey, M. Murindahabi, P. Ringwald, D. A. Fidock, A. Mbituyumuremyi, D. Menard, Emergence and clonal expansion of in vitro artemisinin-resistant *Plasmodium falciparum* kelch13 R561H mutant parasites in Rwanda. *Nat. Med.* **26**, 1602–1608 (2020).
5. M. A. Phillips, J. N. Burrows, C. Manyando, R. H. van Huijsduijnen, W. C. Van Voorhis, T. N. C. Wells, Malaria. *Nat. Rev. Dis. Primers* **3**, 17050 (2017).
6. D. Plouffe, A. Brinker, C. McNamara, K. Henson, N. Kato, K. Kuhen, A. Nagle, F. Adrian, J. T. Matzen, P. Anderson, T. G. Nam, N. S. Gray, A. Chatterjee, J. Janes, S. F. Yan, R. Trager, J. S. Caldwell, P. G. Schultz, Y. Zhou, E. A. Winzeler, In silico activity profiling reveals the mechanism of action of antimalarials discovered in a high-throughput screen. *Proc. Natl. Acad. Sci. U.S.A.* **105**, 9059–9064 (2008).
7. F. J. Gamo, L. M. Sanz, J. Vidal, C. de Cozar, E. Alvarez, J.-L. Lavandera, D. E. Vanderwall, D. V. S. Green, V. Kumar, S. Hasan, J. R. Brown, C. E. Peishoff, L. R. Cardon, J. F. Garcia-Bustos, Thousands of chemical starting points for antimalarial lead identification. *Nature* **465**, 305–310 (2010).
8. W. A. Guiguemde, A. A. Shelat, D. Bouck, S. Duffy, G. J. Crowther, P. H. Davis, D. C. Smithson, M. Connelly, J. Clark, F. Zhu, M. B. Jimenez-Diaz, M. S. Martinez, E. B. Wilson, A. K. Tripathi, J. Gut, E. R. Sharlow, I. Bathurst, F. El Mazouni, J. W. Fowble, I. Forquer, P. L. McGinley, S. Castro, I. Angulo-Barturen, S. Ferrer, P. J. Rosenthal, J. L. Derisi, D. J. Sullivan, J. S. Lazo, D. S. Roos, M. K. Riscoe, M. A. Phillips, P. K. Rathod, W. C. Van Voorhis, V. M. Avery, R. K. Guy, Chemical genetics of *Plasmodium falciparum*. *Nature* **465**, 311–315 (2010).
9. K. Katsuno, J. N. Burrows, K. Duncan, R. Hooft van Huijsduijnen, T. Kaneko, K. Kita, C. E. Mowbray, D. Schmatz, P. Warner, B. T. Slingsby, Hit and lead criteria in drug discovery for infectious diseases of the developing world. *Nat. Rev. Drug Discov.* **14**, 751–758 (2015).
10. H. J. Rupprecht, J. vom Dahl, W. Terres, K. M. Seyfarth, G. Richardt, H. P. Schultheibeta, M. Buerke, F. H. Sheehan, H. Drexler, Cardioprotective effects of the Na^+/H^+ exchange inhibitor cariporide in patients with acute anterior myocardial infarction undergoing direct PTCA. *Circulation* **101**, 2902–2908 (2000).
11. Q. Chen, Y. Liu, X. L. Zhu, F. Feng, H. Yang, W. Xu, Increased NHE1 expression is targeted by specific inhibitor cariporide to sensitize resistant breast cancer cells to doxorubicin in vitro and in vivo. *BMC Cancer* **19**, 211 (2019).
12. L. M. Sanz, B. Crespo, C. De-Cozar, X. C. Ding, J. L. Llergo, J. N. Burrows, J. F. Garcia-Bustos, F. J. Gamo, *P. falciparum in vitro* killing rates allow to discriminate between different antimalarial mode-of-action. *PLOS ONE* **7**, e30949 (2012).
13. N. J. White, Qinghaosu (artemisinin): The price of success. *Science* **320**, 330–334 (2008).
14. I. Angulo-Barturen, M. B. Jimenez-Diaz, T. Mulet, J. Rullas, E. Herreros, S. Ferrer, E. Jimenez, A. Mendoza, J. Regadera, P. J. Rosenthal, I. Bathurst, D. L. Pompliano, F. Gomez de las Heras, D. Gargallo-Viola, A murine model of falciparum-malaria by in vivo selection of competent strains in non-myelodepleted mice engrafted with human erythrocytes. *PLOS ONE* **3**, e2252 (2008).
15. J. M. Murithi, E. S. Owen, E. S. Istvan, M. C. S. Lee, S. Ottilie, K. Chibale, D. E. Goldberg, E. A. Winzeler, M. Llinas, D. A. Fidock, M. Vanaerschot, Combining stage specificity and metabolomic profiling to advance antimalarial drug discovery. *Cell Chem. Biol.* **27**, 158–171.e3 (2020).
16. C. W. McNamara, M. C. Lee, C. S. Lim, S. H. Lim, J. Roland, O. Simon, B. K. Yeung, A. K. Chatterjee, S. L. McCormack, M. J. Manary, A. M. Zeeman, K. J. Dechering, T. S. Kumar, P. P. Henrich, K. Gagaring, M. Ibanez, N. Kato, K. L. Kuhen, C. Fischli, A. Nagle, M. Rottmann, D. M. Plouffe, B. Bursulaya, S. Meister, L. Rameh, J. Trappe, D. Haasen, M. Timmerman, R. W. Sauerwein, R. Suwanarusk, B. Russell, L. Renia, F. Nosten, D. C. Tully, C. H. Kocken, R. J. Glynne, C. Bodenreider, D. A. Fidock, T. T. Diagana, E. A. Winzeler, Targeting *Plasmodium* PI(4)K to eliminate malaria. *Nature* **504**, 248–253 (2013).
17. S. M. Ganesan, A. Falla, S. J. Goldfless, A. S. Nasamu, J. C. Niles, Synthetic RNA-protein modules integrated with native translation mechanisms to control gene expression in malaria parasites. *Nat. Commun.* **7**, 10727 (2016).
18. K. E. Jackson, N. Klonis, D. J. Ferguson, A. Adisa, C. Dogovski, L. Tilley, Food vacuole-associated lipid bodies and heterogeneous lipid environments in the malaria parasite, *Plasmodium falciparum*. *Mol. Microbiol.* **54**, 109–122 (2004).
19. H. G. Elmendorf, K. Haldar, Identification and localization of ERD2 in the malaria parasite *Plasmodium falciparum*: Separation from sites of sphingomyelin synthesis and implications for organization of the Golgi. *EMBO J.* **12**, 4763–4773 (1993).
20. W. H. Witola, G. Pessi, K. El Bissati, J. M. Reynolds, C. B. Mamoun, Localization of the phosphoethanolamine methyltransferase of the human malaria parasite *Plasmodium falciparum* to the Golgi apparatus. *J. Biol. Chem.* **281**, 21305–21311 (2006).
21. J. Birnbaum, S. Scharf, S. Schmidt, E. Jonscher, W. A. M. Hoeijmakers, S. Flemming, C. G. Toenhake, M. Schmitt, R. Sabitzki, B. Bergmann, U. Frohlke, P. Mesen-Ramirez, A. Blancke Soares, H. Herrmann, R. Bartfai, T. Spielmann, A Kelch13-defined endocytosis pathway mediates artemisinin resistance in malaria parasites. *Science* **367**, 51–59 (2020).
22. N. F. Gnadig, B. H. Stokes, R. L. Edwards, G. F. Kalantarov, K. C. Heimsch, M. Kuderjavy, A. Crane, M. C. S. Lee, J. Straimer, K. Becker, I. N. Trakht, A. R. Odom John, S. Mok, D. A. Fidock, Insights into the intracellular localization, protein associations and artemisinin resistance properties of *Plasmodium falciparum* K13. *PLOS Pathog.* **16**, e1008482 (2020).
23. A. R. Demas, A. I. Sharma, W. Wong, A. M. Early, S. Redmond, S. Bopp, D. E. Neafsey, S. K. Volkman, D. L. Hartl, D. F. Wirth, Mutations in *Plasmodium falciparum* actin-binding protein coronin confer reduced artemisinin susceptibility. *Proc. Natl. Acad. Sci. U.S.A.* **115**, 12799–12804 (2018).
24. N. B. Miliaras, B. Wendland, EH proteins: Multivalent regulators of endocytosis (and other pathways). *Cell Biochem. Biophys.* **41**, 295–318 (2004).
25. B. Blasco, D. Leroy, D. A. Fidock, Antimalarial drug resistance: Linking *Plasmodium falciparum* parasite biology to the clinic. *Nat. Med.* **23**, 917–928 (2017).
26. M. Rottmann, C. McNamara, B. K. Yeung, M. C. Lee, B. Zou, B. Russell, P. Seitz, D. M. Plouffe, N. V. Dharia, J. Tan, S. B. Cohen, K. R. Spencer, G. E. Gonzalez-Paez, S. B. Lakshminarayana, A. Goh, R. Suwanarusk, T. Jegla, E. K. Schmitt, H. P. Beck, R. Brun, F. Nosten, L. Renia, V. Dartois, T. H. Keller, D. A. Fidock, E. A. Winzeler, T. T. Diagana, Spiroindolones, a potent compound class for the treatment of malaria. *Science* **329**, 1175–1180 (2010).
27. B. Baragana, I. Hallyburton, M. C. Lee, N. R. Norcross, R. Grimaldi, T. D. Otto, W. R. Proto, A. M. Blagborough, S. Meister, G. Wirjanata, A. Ruecker, L. M. Upton, T. S. Abraham, M. J. Almeida, A. Pradhan, A. Porzelle, T. Luksch, M. S. Martinez, T. Luksch, J. M. Bolscher, A. Woodland, S. Norval, F. Zuccotto, J. Thomas, F. Simeons, L. Stojanovski, M. Osuna-Cabello, P. M. Brock, T. S. Churcher, K. A. Sala, S. E. Zakutansky, M. B. Jimenez-Diaz, L. M. Sanz, J. Riley, R. Basak, M. Campbell, V. M. Avery, R. W. Sauerwein, K. J. Dechering, R. Noviyanti, B. Campo, J. A. Frearson, I. Angulo-Barturen, S. Ferrer-Bazaga, F. J. Gamo, P. G. Wyatt, D. Leroy, P. Siegl, M. J. Delves, D. E. Kyle, S. Wittlin, J. Marfurt, R. N. Price, R. E. Sinden, E. A. Winzeler, S. A. Charman, L. Bebrevska, D. W. Gray, S. Campbell, A. H. Fairlamb, P. A. Willis, J. C. Rayner, D. A. Fidock, K. D. Read, I. H. Gilbert, A novel multiple-stage antimalarial agent that inhibits protein synthesis. *Nature* **522**, 315–320 (2015).
28. A. H. Lee, D. A. Fidock, Evidence of a mild mutator phenotype in Cambodian *Plasmodium falciparum* malaria parasites. *PLOS ONE* **11**, e0154166 (2016).
29. X. C. Ding, D. Ubben, T. N. Wells, A framework for assessing the risk of resistance for anti-malarials in development. *Malar. J.* **11**, 292 (2012).
30. S. E. Bopp, M. J. Manary, A. T. Bright, G. L. Johnston, N. V. Dharia, F. L. Luna, S. McCormack, D. Plouffe, C. W. McNamara, J. R. Walker, D. A. Fidock, E. L. Denchi, E. A. Winzeler, Mitotic evolution of *Plasmodium falciparum* shows a stable core genome but recombination in antigen families. *PLOS Genet.* **9**, e1003293 (2013).
31. A. Claessens, W. L. Hamilton, M. Kekre, T. D. Otto, A. Faizullabhoy, J. C. Rayner, D. Kwiatkowski, Generation of antigenic diversity in *Plasmodium falciparum* by structured rearrangement of *var* genes during mitosis. *PLOS Genet.* **10**, e1004812 (2014).
32. M. Zhang, C. Wang, T. D. Otto, J. Oberstaller, X. Liao, S. R. Adapa, K. Udenze, I. F. Bronner, D. Casandra, M. Mayho, J. Brown, S. Li, J. Swanson, J. C. Rayner, R. H. Y. Jiang, J. H. Adams,

Uncovering the essential genes of the human malaria parasite *Plasmodium falciparum* by saturation mutagenesis. *Science* **360**, eaap7847 (2018).
33. V. Thakur, M. Asad, S. Jain, M. E. Hossain, A. Gupta, I. Kaur, S. Rathore, S. Ali, N. J. Khan, A. Mohmmed, Eps15 homology domain containing protein of *Plasmodium falciparum* (PfEHD) associates with endocytosis and vesicular trafficking towards neutral lipid storage site. *Biochim. Biophys. Acta* **1853**, 2856–2869 (2015).
34. R. C. Henrici, R. L. Edwards, M. Zoltner, D. A. van Schalkwyk, M. N. Hart, F. Mohring, R. W. Moon, S. D. Nofal, A. Patel, C. Flueck, D. A. Baker, A. R. Odom John, M. C. Field, C. J. Sutherland, The *Plasmodium falciparum* artemisinin susceptibility-associated AP-2 adaptin μ subunit is clathrin independent and essential for schizont maturation. *mBio* **11**, e02918–e02919 (2020).
35. T. Yang, S. Ottilie, E. S. Istvan, K. P. Godinez-Macias, A. K. Lukens, B. Baragana, B. Campo, C. Walpole, J. C. Niles, K. Chibale, K. J. Dechering, M. Llinas, M. C. S. Lee, N. Kato, S. Wyllie, C. W. McNamara, F. J. Gamo, J. Burrows, D. A. Fidock, D. E. Goldberg, I. H. Gilbert, D. F. Wirth, E. A. Winzeler; Malaria Drug Accelerator Consortium, MalDA, accelerating malaria drug discovery. *Trends Parasitol.* **37**, 493–507 (2021).
36. C. Snyder, J. Chollet, J. Santo-Tomas, C. Scheurer, S. Wittlin, In vitro and in vivo interaction of synthetic peroxide RBx11160 (OZ277) with piperaquine in *Plasmodium* models. *Exp. Parasitol.* **115**, 296–300 (2007).
37. J. Marfurt, F. Chalfein, P. Prayoga, F. Wabiser, E. Kenangalem, K. A. Piera, D. P. Fairlie, E. Tjitra, N. M. Anstey, K. T. Andrews, R. N. Price, Ex vivo activity of histone deacetylase inhibitors against multidrug-resistant clinical isolates of *Plasmodium falciparum* and *P. vivax*. *Antimicrob. Agents Chemother.* **55**, 961–966 (2011).
38. J. Marfurt, F. Chalfein, P. Prayoga, F. Wabiser, E. Kenangalem, K. A. Piera, B. Machunter, E. Tjitra, N. M. Anstey, R. N. Price, Ex vivo drug susceptibility of ferroquine against chloroquine-resistant isolates of *Plasmodium falciparum* and *P. vivax*. *Antimicrob. Agents Chemother.* **55**, 4461–4464 (2011).
39. B. Russell, F. Chalfein, B. Prasetyorini, E. Kenangalem, K. Piera, R. Suwanarusk, A. Brockman, P. Prayoga, P. Sugiarto, Q. Cheng, E. Tjitra, N. M. Anstey, R. N. Price, Determinants of in vitro drug susceptibility testing of *Plasmodium vivax*. *Antimicrob. Agents Chemother.* **52**, 1040–1045 (2008).
40. M. Smilkstein, N. Sriwilaijaroen, J. X. Kelly, P. Wilairat, M. Riscoe, Simple and inexpensive fluorescence-based technique for high-throughput antimalarial drug screening. *Antimicrob. Agents Chemother.* **48**, 1803–1806 (2004).
41. S. H. Adjalley, G. L. Johnston, T. Li, R. T. Eastman, E. H. Ekland, A. G. Eappen, A. Richman, B. K. Sim, M. C. S. Lee, S. L. Hoffman, D. A. Fidock, Quantitative assessment of *Plasmodium falciparum* sexual development reveals potent transmission-blocking activity by methylene blue. *Proc. Natl. Acad. Sci. U.S.A.* **108**, E1214–E1223 (2011).
42. M. Vanaerschot, L. Lucantoni, T. Li, J. M. Combrinck, A. Ruecker, T. R. S. Kumar, K. Rubiano, P. E. Ferreira, G. Siciliano, S. Gulati, P. P. Henrich, C. L. Ng, J. M. Murithi, V. C. Corey, S. Duffy, O. J. Lieberman, M. I. Veiga, R. E. Sinden, P. Alano, M. J. Delves, K. L. Sim, E. A. Winzeler, T. J. Egan, S. L. Hoffman, V. M. Avery, D. A. Fidock, Hexahydroquinolines are antimalarial candidates with potent blood-stage and transmission-blocking activity. *Nat. Microbiol.* **2**, 1403–1414 (2017).
43. E. H. Ekland, J. Schneider, D. A. Fidock, Identifying apicoplast-targeting antimalarials using high-throughput compatible approaches. *FASEB J.* **25**, 3583–3593 (2011).
44. M. Vanaerschot, J. M. Murithi, C. F. A. Pasaje, S. Ghidelli-Disse, L. Dwomoh, M. Bird, N. Spottiswoode, N. Mittal, L. B. Arendse, E. S. Owen, K. J. Wicht, G. Siciliano, M. Bosche, T. Yeo, T. R. S. Kumar, S. Mok, E. F. Carpenter, M. J. Giddins, O. Sanz, S. Ottilie, P. Alano, K. Chibale, M. Llinas, A. C. Uhlemann, M. Delves, A. B. Tobin, C. Doerig, E. A. Winzeler, M. C. S. Lee, J. C. Niles, D. A. Fidock, Inhibition of resistance-refractory *P. falciparum* kinase PKG delivers prophylactic, blood stage, and transmission-blocking antiplasmodial activity. *Cell Chem. Biol.* **27**, 806–816.e8 (2020).
45. E. Yoo, C. J. Schulze, B. H. Stokes, O. Onguka, T. Yeo, S. Mok, N. F. Gnadig, Y. Zhou, K. Kurita, I. T. Foe, S. M. Terrell, M. J. Boucher, P. Cieplak, K. Kumpornsin, M. C. S. Lee, R. G. Linington, J. Z. Long, A. C. Uhlemann, E. Weerapana, D. A. Fidock, M. Bogyo, The antimalarial natural product Salinipostin A identifies essential α/β serine hydrolases involved in lipid metabolism in *P. falciparum* parasites. *Cell Chem. Biol.* **27**, 143–157.e5 (2020).
46. D. A. Fidock, T. Nomura, T. E. Wellems, Cycloguanil and its parent compound proguanil demonstrate distinct activities against *Plasmodium falciparum* malaria parasites transformed with human dihydrofolate reductase. *Mol. Pharmacol.* **54**, 1140–1147 (1998).
47. S. H. Adjalley, M. C. Lee, D. A. Fidock, A method for rapid genetic integration into *Plasmodium falciparum* utilizing mycobacteriophage Bxb1 integrase. *Methods Mol. Biol.* **634**, 87–100 (2010).
48. C. B. Mamoun, I. Y. Gluzman, S. Goyard, S. M. Beverley, D. E. Goldberg, A set of independent selectable markers for transfection of the human malaria parasite *Plasmodium falciparum*. *Proc. Natl. Acad. Sci. U.S.A.* **96**, 8716–8720 (1999).
49. P. Wang, Q. Wang, P. F. Sims, J. E. Hyde, Rapid positive selection of stable integrants following transfection of *Plasmodium falciparum*. *Mol. Biochem. Parasitol.* **123**, 1–10 (2002).
50. D. A. Fidock, T. E. Wellems, Transformation with human dihydrofolate reductase renders malaria parasites insensitive to WR99210 but does not affect the intrinsic activity of proguanil. *Proc. Natl. Acad. Sci. U.S.A.* **94**, 10931–10936 (1997).
51. A. S. Nasamu, A. Falla, C. F. A. Pasaje, B. A. Wall, J. C. Wagner, S. M. Ganesan, S. J. Goldfless, J. C. Niles, An integrated platform for genome engineering and gene expression perturbation in *Plasmodium falciparum*. *Sci. Rep.* **11**, 342 (2021).
52. K. Deitsch, C. Driskill, T. Wellems, Transformation of malaria parasites by the spontaneous uptake and expression of DNA from human erythrocytes. *Nucleic Acids Res.* **29**, 850–853 (2001).
53. D. A. Fidock, T. Nomura, A. K. Talley, R. A. Cooper, S. M. Dzekunov, M. T. Ferdig, L. M. Ursos, A. B. Sidhu, B. Naude, K. W. Deitsch, X. Z. Su, J. C. Wootton, P. D. Roepe, T. E. Wellems, Mutations in the *P. falciparum* digestive vacuole transmembrane protein PfCRT and evidence for their role in chloroquine resistance. *Mol. Cell* **6**, 861–871 (2000).
54. M. Karyana, L. Burdarm, S. Yeung, E. Kenangalem, N. Wariker, R. Maristela, K. G. Umana, R. Vemuri, M. J. Okoseray, P. M. Penttinen, P. Ebsworth, P. Sugiarto, N. M. Anstey, E. Tjitra, R. N. Price, Malaria morbidity in Papua Indonesia, an area with multidrug resistant *Plasmodium vivax* and *Plasmodium falciparum*. *Malar. J.* **7**, 148 (2008).
55. A. F. Cowman, S. Karcz, D. Galatis, J. G. Culvenor, A P-glycoprotein homologue of *Plasmodium falciparum* is localized on the digestive vacuole. *J. Cell Biol.* **113**, 1033–1042 (1991).
56. G. Cremer, L. K. Basco, J. Le Bras, D. Camus, C. Slomianny, *Plasmodium falciparum*: Detection of P-glycoprotein in chloroquine-susceptible and chloroquine-resistant clones and isolates. *Exp. Parasitol.* **81**, 1–8 (1995).
57. M. Klemba, W. Beatty, I. Gluzman, D. E. Goldberg, Trafficking of plasmepsin II to the food vacuole of the malaria parasite *Plasmodium falciparum*. *J. Cell Biol.* **164**, 47–56 (2004).
58. P. N. Tran, S. H. Brown, M. Rug, M. C. Ridgway, T. W. Mitchell, A. G. Maier, Changes in lipid composition during sexual development of the malaria parasite *Plasmodium falciparum*. *Malar. J.* **15**, 73 (2016).
59. N. M. Palacpac, Y. Hiramine, F. Mi-ichi, M. Torii, K. Kita, R. Hiramatsu, T. Horii, T. Mitamura, Developmental-stage-specific triacylglycerol biosynthesis, degradation and trafficking as lipid bodies in *Plasmodium falciparum*-infected erythrocytes. *J. Cell Sci.* **117**, 1469–1480 (2004).
60. K. S. Bane, S. Lepper, J. Kehrer, J. M. Sattler, M. Singer, M. Reinig, D. Klug, K. Heiss, J. Baum, A. K. Mueller, F. Frischknecht, The actin filament-binding protein coronin regulates motility in *Plasmodium* sporozoites. *PLOS Pathog.* **12**, e1005710 (2016).
61. J. R. Gallagher, S. T. Prigge, *Plasmodium falciparum* acyl carrier protein crystal structures in disulfide-linked and reduced states and their prevalence during blood stage growth. *Proteins* **78**, 575–588 (2010).
62. E. Mouray, M. Moutiez, S. Girault, C. Sergheraert, I. Florent, P. Grellier, Biochemical properties and cellular localization of *Plasmodium falciparum* protein disulfide isomerase. *Biochimie* **89**, 337–346 (2007).
63. A. Wandinger-Ness, M. Zerial, Rab proteins and the compartmentalization of the endosomal system. *Cold Spring Harb. Perspect. Biol.* **6**, a022616 (2014).
64. H. Stenmark, Rab GTPases as coordinators of vesicle traffic. *Nat. Rev. Mol. Cell Biol.* **10**, 513–525 (2009).
65. J. Kim, Y. Z. Tan, K. J. Wicht, S. K. Erramilli, S. K. Dhingra, J. Okombo, J. Vendome, L. M. Hagenah, S. I. Giacometti, A. L. Warren, K. Nosol, P. D. Roepe, C. S. Potter, B. Carragher, A. A. Kossiakoff, M. Quick, D. A. Fidock, F. Mancia, Structure and drug resistance of the *Plasmodium falciparum* transporter PfCRT. *Nature* **576**, 315–320 (2019).
66. C. Marin-Mogollon, A. M. Salman, K. M. J. Koolen, J. M. Bolscher, F. J. A. van Pul, S. Miyazaki, T. Imai, A. S. Othman, J. Ramesar, G. J. van Gemert, H. Kroeze, S. Chevalley-Maurel, B. Franke-Fayard, R. W. Sauerwein, A. V. S. Hill, K. J. Dechering, C. J. Janse, S. M. Khan, A *P. falciparum* NF54 reporter line expressing mCherry-luciferase in gametocytes, sporozoites, and liver-stages. *Front. Cell. Infect. Microbiol.* **9**, 96 (2019).
67. M. J. Delves, U. Straschil, A. Ruecker, C. Miguel-Blanco, S. Marques, A. C. Dufour, J. Baum, R. E. Sinden, Routine in vitro culture of *P. falciparum* gametocytes to evaluate novel transmission-blocking interventions. *Nat. Protoc.* **11**, 1668–1680 (2016).

Acknowledgments: We thank D. Leboulleux (Sanofi, now Evotec), A. Laso, and E. Ochoa from AleoVitro SL for their contribution to this study. We thank J. Prakash (Syngene) for the synthesis of the compounds, and C. Scheurer, S. Sax, and C. Fischli (Swiss TPH) for the generation of in vitro parasitology data. We are grateful to K. Dechering (TropIQ Health Sciences) and M. Delves (London School of Hygiene and Tropical Medicine) for providing *P. falciparum* liver and sexual stage data, respectively. We also thank J. N. Burrows and other MMV colleagues for critical review of the manuscript. **Funding:** Funding for this work was provided by the Medicines for Malaria Venture and in-kind contribution from Sanofi. D.A.F. gratefully acknowledges funding support from the NIH (R01 AI124678, R01 AI109023), the Bill & Melinda Gates Foundation (OPP1201387), and the Department of Defense (W81XWH-19-1-0086). S.M. is grateful for support from a Human Frontier Science Program Long-term Postdoctoral Fellowship LT000976/2016-L. R.N.P. was supported by a Wellcome Trust Senior Fellowship in Clinical Science (200909). **Author contributions:** J.M.M., C.P., I.A.-B.,

G.C., L.F., A.P., D.A.F., and D.L. designed the study. J.M.M., J.B., N.F.G., C.F.A.P., K.R., P.D., M.B.J.-D., J. Marfurt, G.W., R.N., and P.T. generated data. J.M.M., C.P., J.B., X.B., N.F.G., C.F.A.P., K.R., T.Y., S.M., S.K., P.D., M.B.J.-D., J. Marfurt, D.B., M.H.C.-R., N.G., S.W., R.N.P., G.W., R.N., P.T., R.A.C., P.J.R., L.M.S., F.J.G., J.M.A., E.G., T.B., T.V., G.T., J.-M.G., M.F.N., N.B., I.A.-B., F.E., D.A.F., and D.L. analyzed data. C.P., X.B., A.-C.U., R.A.C., J.J., S.S., S.B., J. Menegotto, L.S., G.L., M.-J.C., I.A.-B., B.B., and J.C.N. provided reagents or expertise. M.R., M.D., R.M., L.B., B.B., S.C., G.C., L.F., A.P., D.A.F., and D.L. were the project managers. J.M.M., D.A.F. and D.L. wrote the manuscript, with input from all the authors. Medicinal–synthetic chemistry/drug discovery: C.P., D.B., M.R., J.J., S.S., S.B., N.B., I.A.-B., F.E., B.B., S.C., G.C., L.F., A.P., and D.L. Preclinical ADME/PK-PD studies, modeling, and bioinformatics: X.B., S.K., M.B.J.-D., M.H.C.-R., N.G., S.W., E.G., T.B., T.V., G.T., and I.A.-B. Toxicology and safety studies: P.D. and M.D. Molecular biology, microscopy, in vitro parasitology, and field isolate studies: J.M.M., J.B., N.F.G., C.F.A.P., K.R., T.Y., S.M., A.-C.U., J.N., D.A.F., D.L., J. Marfurt, S.W., R.N.P., G.W., R.N., P.T., R.A.C., P.J.R., L.M.S., F.J.G., J.M.A., and B.B. Translational sciences, developability/API: J. Menegotto, L.S., G.L., M.-J.C., M.F.N., and L.B. **Competing interests:** M.R., M.H.C.-R., N.G., D.B., L.B., F.E., S.C., and D.L. are employees of MMV. B.B. was successively an employee of and a paid consultant for MMV. At the time of the study, C.P., X.B., P.D., S.K., J.M.A., E.G., T.B., T.V., G.T., J.-M.G., J. Menegotto, L.S., G.L., M.-J.C., M.F.N., M.D., R.M., N.B., L.F., and A.P. were employees of Sanofi. L.M.S. and F.J.G. are employees of GSK. J.J., S.S., and S.B. are employees of Syngene. G.C. is an employee of Bioaster. M.B.J.-D. and I.A.-B. are shareholders of the Art of Discovery. All other authors declare that they have no competing interests. C.P., A.P., G.C., and S.C. are authors on the MMV688533 patent WO2019008027A1 (PCT/EP2018/068079). **Data and materials availability:** All data associated with this study are present in the paper or the Supplementary Materials. Requests for resources and reagents including compounds should be directed to the corresponding authors D.L. (leroyd@mmv.org) or D.F. (df2260@cumc.columbia.edu). MMV688533 is available upon contacting D.L. and under a material transfer agreement that will be established between the requestor's institution and Medicines for Malaria Venture.

Submitted 15 January 2021
Accepted 2 July 2021
Published 21 July 2021
10.1126/scitranslmed.abg6013

Citation: J. M. Murithi, C. Pascal, J. Bath, X. Boulenc, N. F. Gnädig, C. F. Pasaje, K. Rubiano, T. Yeo, S. Mok, S. Klieber, P. Desert, M. B. Jimenez-Diaz, J. Marfurt, M. Rouillier, M. H. Cherkaoui-Rbati, N. Gobeau, S. Wittlin, A.-C. Uhlemann, R. N. Price, G. Wirjanata, R. Noviyanti, P. Tumwebaze, R. A. Cooper, P. J. Rosenthal, L. M. Sanz, F. J. Gamo, J. Joseph, S. Singh, S. Bashyam, J. M. Augereau, E. Giraud, T. Bozec, T. Vermat, G. Tuffal, J.-M. Guillon, J. Menegotto, L. Sallé, G. Louit, M.-J. Cabanis, M. F. Nicolas, M. Doubovetzky, R. Merino, N. Bessila, I. Angulo-Barturen, D. Baud, L. Bebrevska, F. Escudié, J. C. Niles, B. Blasco, S. Campbell, G. Courtemanche, L. Fraisse, A. Pellet, D. A. Fidock, D. Leroy, The antimalarial MMV688533 provides potential for single-dose cures with a high barrier to *Plasmodium falciparum* parasite resistance. *Sci. Transl. Med.* **13**, eabg6013 (2021).

Science Translational Medicine

The antimalarial MMV688533 provides potential for single-dose cures with a high barrier to *Plasmodium falciparum* parasite resistance

James M. MurithiCécile PascalJade BathXavier BoulencNina F. GnädigCharisse Flerida A. PasajeKelly RubianoTomas YeoSachel MokSylvie KlieberPaul DesertMaría Belén Jiménez-DíazJutta MarfurtMélanie RouillierMohammed H. Cherkaoui-RbatiNathalie GobeauSergio WittlinAnne-Catrin UhlemannRic N. PriceGrennady WirjanataRintis NoviyantiPatrick TumwebazeRoland A. CooperPhilip J. RosenthalLaura M. SanzFrancisco Javier GamoJayan JosephShivendra SinghSridevi BashyamJean Michel AugereauElie GiraudTanguy BozecThierry VermatGilles TuffalJean-Michel GuillonJérôme MenegottoLaurent SalléGuillaume LouitMarie-José CabanisMarie Françoise NicolasMichel DoubovetzkyRita MerinoNadir BessilaIñigo Angulo-BarturenDelphine BaudLidiya BebrevskaFanny EscudiéJacquin C. NilesBenjamin BlascoSimon CampbellGilles CourtemancheLaurent FraisseAlain PelletDavid A. FidockDidier Leroy

Sci. Transl. Med., 13 (603), eabg6013. • DOI: 10.1126/scitranslmed.abg6013

Antimalarial advance

The need for antimalarial drugs is urgent in the face of growing resistance to existing therapies. Murithi *et al.* characterized MMV688533, an acylguanidine identified from compounds inhibiting known human drug targets that were screened for activity against *Plasmodium falciparum*. MMV688533 showed rapid in vitro killing of multiple *P. falciparum* strains as well as *P. vivax*. A single dose of MMV688533 rapidly reduced parasitemia in a *P. falciparum* NSG mouse model of infection, and this agent displayed favorable pharmacokinetic and toxicity profiles. MMV688533 selected for only low-grade resistance, with resistant parasites remaining sensitive to existing antimalarials. These findings suggest that MMV688533 is a promising antimalarial candidate with a low resistance risk and the promise of a single-dose cure, which merits further study.